The Journal of Physiology

https://jp.msubmit.net

JP-RP-2019-279203R1

Title: TRESK background K+ channel deletion selectively uncovers enhanced mechanical and cold sensitivity

Authors: Aida Castellanos
Anna Pujol-Coma
Alba Andres-Bilbe
Ahmed Negm
Gerard Callejo
David Soto
Jacques Noel
Nuria Comes
Xavier Gasull

Author Conflict: No competing interests declared

Author Contribution: Aida Castellanos: Conception or design of the work; Final approval of the version to be published Anna Pujol-Coma: Acquisition or analysis or interpretation of data for the work Alba Andres-Bilbe: Acquisition or analysis or interpretation of data for the work Ahmed Negm: Acquisition or analysis or interpretation of data for the work Gerard Callejo: Conception or design of the work; Acquisition or analysis or interpretation of data for the work David Soto: Acquisition or analysis or interpretation of data for the work; Drafting the work or revising it critically for important intellectual content; Final approval of the version to be published Jacques Noel: Conception or design of the work; Acquisition or analysis or interpretation of data for the work; Drafting the work or revising it critically for important intellectual content;

Final approval of the version to be published Nuria Comes: Acquisition or analysis or interpretation of data for the work; Drafting the work or revising it critically for important intellectual content; Final approval of the version to be published Xavier Gasull: Conception or design of the work; Acquisition or analysis or interpretation of data for the work; Drafting the work or revising it critically for important intellectual content; Final approval of the version to be published; Agreement to be accountable for all aspects of the work

Running Title: TRESK modulation of mechanical and cold sensitivity

Dual Publication: No

Funding: Ministry of Economy and Competitiveness | Instituto de Salud Carlos III (Carlos III Health Institute): Xavier Gasull, FIS PI14/00141; Ministry of Economy and Competitiveness | Instituto de Salud Carlos III (Carlos III Health Institute): Xavier Gasull, FIS PI17/00296; Ministry of Economy and Competitiveness | Instituto de Salud Carlos III (Carlos III Health Institute): David Soto, Nuria Comes, Xavier Gasull, RETICs Oftared RD16/0008/0014; Ministerio de Ciencia e Innovación (MICINN): David Soto, BFU2017-83317-P; Generalitat de Catalunya (Government of Catalonia): David Soto, Nuria Comes, Xavier Gasull, 2017SGR737; Maria de Maeztu, Institut de Neurociencies UB (UBNeuro): Xavier Gasull, MDM-2017-0729

TRESK background K^+ channel deletion selectively uncovers enhanced mechanical and cold sensitivity

Aida Castellanos[1,2], Anna Pujol-Coma[1,2], Alba Andres-Bilbe[1,2], Ahmed Negm[3,4], Gerard Callejo[1], David Soto[1,2], Jacques Noël[3,4], Nuria Comes[1,2] and Xavier Gasull[1,2]

[1] Neurophysiology Laboratory, Department of Biomedicine, Medical School, Institute of Neurosciences, Universitat de Barcelona, 08036 Barcelona, Spain
[2] Institut d'Investigacions Biomèdiques August Pi i Sunyer (IDIBAPS), 08036 Barcelona, Spain
[3]Université Côte d'Azur, CNRS UMR 7275, Institut de Pharmacologie Moléculaire et Cellulaire, Valbonne, France
[4]LabEx Ion Channel Science and Therapeutics, Valbonne, France.

Abbreviated title: TRESK modulation of mechanical and cold sensitivity

Corresponding author:
Xavier Gasull, Ph.D.
Dept. Biomedicina-Fisiologia
Facultat de Medicina
Universitat de Barcelona
Casanova 143
E-08036 Barcelona
Spain

Tel: (+34) 934.024.519
E-mail: xgasull@ub.edu

Num. of pages: 58
6 Figures

Author profile

Aida Castellanos received her degree in Biology from the University of Girona, Spain. She subsequently got her Master's Degree in Neuroscience from the University of Barcelona, Spain, and then joined the Neurophysiology Group at the same University. She got her PhD in the field of somatosensation and pain characterizing ion channels involved in the regulation of nociceptor excitability. Currently, she holds a postdoctoral position at the Physiology Group of the University of Barcelona, where she studies the physiopathological relationship between glia and neurons, with a particular interest in rare diseases.

Footnote - Preprint publication

This article was first published as a preprint: Castellanos A, Pujol-Coma A, Andres-Bilbe A, Negm A, Callejo G, Soto D, Noël J, Comes N, Gasull X. (2019). TRESK background K^+ channel deletion selectively uncovers enhanced mechanical and cold sensitivity. bioRxiv. https://doi.org/10.1101/636829

Key points summary

- TRESK background K^+ channel is expressed in sensory neurons and acts as a brake to reduce neuronal activation.
- Deletion of the channel enhances the excitability of nociceptors
- Skin nociceptive C-fibers show an enhanced activation by cold and mechanical stimulation in TRESK KO animals.
- Channel deletion selectively enhances mechanical and cold sensitivity in mice, without altering sensitivity to heat.
- These results indicate that the channel regulates the excitability of specific neuronal subpopulations involved in mechanosensitivity and cold-sensing.

Abstract

Background potassium-permeable ion channels play a critical role in tuning the excitability of nociceptors, yet the precise role played by different subsets of channels is not fully understood. Decreases in TRESK (TWIK-related spinal cord K^+ channel) expression/function enhance sensory neurons excitability, but its role in somatosensory perception and nociception is poorly understood. Here, we used a TRESK knockout (KO) mouse to address these questions. We show that TRESK regulates the sensitivity of sensory neurons in a modality-specific manner, contributing to mechanical and cold sensitivity but without any effect on heat sensitivity. Nociceptive neurons isolated from TRESK KO mice show a decreased threshold for activation and skin nociceptive C-fibers show an enhanced activation by cold and mechanical stimulation that was also observed in behavioral tests in vivo. TRESK is also involved in osmotic pain and in early phases of formalin-induced inflammatory pain, but not in the development of mechanical and heat hyperalgesia during chronic pain. In contrast, mice lacking TRESK present cold allodynia that is not further enhanced by oxaliplatin. In summary, genetic removal of TRESK uncovers enhanced mechanical and cold sensitivity, indicating that the channel regulates the excitability of specific neuronal subpopulations involved in mechanosensitivity and cold-sensing, acting as a brake to prevent activation by innocuous stimuli.

Introduction

The combined activation of depolarizing and hyperpolarizing ion channels determines the likelihood of excitation and generation of action potentials in specific subtypes of sensory neurons such as thermoreceptors, mechanoreceptors or nociceptors. Each subtype present a characteristic pattern of expression of ion channels that define their intrinsic physiological properties such as firing pattern and action potential characteristics (Zheng *et al.*, 2019). Two-pore domain potassium channels (K_{2P}) are expressed in different subpopulations of sensory neurons, including nociceptors where they carry most of the "leak" or background hyperpolarizing current (Enyedi & Czirják, 2010). Their electrophysiological properties allow them to carry K^+ currents over a wide range of membrane potentials and hence they are key determinants of neuronal excitability, decreasing the probability of depolarizing stimuli to reach action potential threshold, as well as shaping the neuron firing response (Enyedi & Czirják, 2010). TRESK (TWIK-related spinal cord K^+ channel), along with other K_{2P} family members TREK-1, TREK-2 and TRAAK channels, generate the major contribution to leak currents in trigeminal (TG) and dorsal root ganglion (DRG) neurons (Patel *et al.*, 1998; Kang & Kim, 2006; Dobler *et al.*, 2007; Yamamoto *et al.*, 2009; Tulleuda *et al.*, 2011), These channels have been implicated in pain perception induced by mechanical, thermal and chemical stimuli, as well as in neuropathic and inflammatory pain (Alloui *et al.*, 2006; Noël *et al.*, 2009; Tulleuda *et al.*, 2011; Marsh *et al.*, 2012; Acosta *et al.*, 2014; Pereira *et al.*, 2014). The modulatory effect that these channels will exert on nociceptors will depend on their expression pattern and their individual properties. Indeed, deletion of one of the K_{2P} channels enhances the specific

sensitivity to certain external stimuli but not others, rather than exerting a general brake on neuronal excitability by decreasing the total K^+ current. In humans, rats and mice, TRESK shows a high expression in DRG and TG neurons and is particularly enriched in sensory ganglia compared to other neural and non-neural tissues (Kang & Kim, 2006; Dobler *et al.*, 2007; Marsh *et al.*, 2012; Manteniotis *et al.*, 2013; Flegel *et al.*, 2015; Usoskin *et al.*, 2015; Ray *et al.*, 2018; Zeisel *et al.*, 2018). Single-cell RNA sequencing data has provided further insight on the role of TRESK, showing that it is present in a subpopulation of low-threshold mechanoreceptors involved in touch sensation (expressing TRKB and Piezo2) and, predominantly, in non-peptidergic nociceptors (Usoskin *et al.*, 2015; Zeisel *et al.*, 2018; Zheng *et al.*, 2019). Interestingly, TRESK expression is down-regulated in different pain conditions, comprising sciatic nerve axotomy (Tulleuda *et al.*, 2011), spared nerve injury (Zhou *et al.*, 2013) and chronic inflammation (Marsh *et al.*, 2012), contributing, together with other changes, to enhance neuronal excitability. In contrast, increasing TRESK expression resulted in a decrease in neuronal excitability and amelioration of painful behaviors (Zhou *et al.*, 2012; 2013; Guo & Cao, 2014). Similarly, mice with a loss-of-function mutation in TRESK [G339R] showed a significant reduction of outward K^+ current, increased excitability and reduced rheobase (Dobler *et al.*, 2007). Furthermore, a frameshift mutation leading to the truncation of the channel has been associated with familial migraine with aura, thus involving TRESK in the enhanced activation of the trigeminovascular system and the release of inflammatory neuropeptides in the meninges and cerebral vessels triggering migraine pain (Lafrenière *et al.*, 2010). This is supported by a recent study demonstrating that mutant TRESK can

heteromerize with TREK-1/2 to decrease their function and trigger migraine pain (Royal *et al.*, 2019).

Despite the fact that TRESK shares some functional properties with other K_{2P} channels, its high expression in sensory neurons points to a relevant and yet unexplored role in sensory perception and pain. We report that TRESK removal uncovers enhanced cold and mechanical sensitivity without affecting thermal sensitivity to warm or hot temperatures.

Methods

Animals

All behavioral and experimental procedures were carried out in accordance with the recommendations of the International Association for the Study of Pain (IASP) and were reviewed and approved by the Animal Care Committee of the University of Barcelona and by the Department of the Environment of the *Generalitat de Catalunya*, Catalonia, Spain (#8466, 8468, 8548, 6869, 9876). Female and male C57BL/6N mice between 8 and 15 weeks old were used in all experimental procedures (RNA extraction and qPCR, cell cultures, electrophysiology, calcium imaging, nerve fiber recording and behavior) unless differentially indicated. Mice were housed at 22ºC with free access to food and water in an alternating 12h light and dark cycle.

TRESK (Kcnk18/K2P18.1) knockout mice (KO) and wild-type (WT) littermates were obtained from the KOMP Repository (Mouse Biology Program, University of California, Davis, CA). The TRESK knockout mouse was generated by replacing the complete Kcnk18 gene by a ZEN-UB1 cassette according to the VelociGene's KOMP Definitive Null Allele Design. At 3 weeks of age, WT or KO newborn mice were weaned, separated, and identified by ear punching. Genomic DNA was isolated from tail snip samples with Maxwell® Mouse Tail DNA Purification Kit (Promega, Madison, WI). Polymerase chain reaction (PCR) was performed with primers to detect the Kcnk18 gene: forward 5'-ACCAACACCAAGCTGTCTTGTTTCTC-3' and reverse 5'-AGACAGATGGACGGACAGACATAGATG-3' or the inserted cassette in the KO mice: forward (REG-Neo-F) 5'-GCAGCCTCTGTTCCACATACACTTCA-3' and

reverse (gene-specific) 5'-AGACTTCTCCCAGGTAACAACTCTGC-3'. The PCR mixture contained 1 µl DNA sample, 2.5 µl PCR buffer (10x concentration), 2 µl dNTP mixture (2.5 mM), 0.5 µl (20 µM) forward and reverse primers, 0.2 µl Taq DNA polymerase (5 U/µl), 1.7 µl $MgCl_2$ (25 mM), 6.5 µl Betaine (5 M), 0.325 µl DMSO and 9.7 µl water (final volume of 25 µl). PCR amplifications were carried out with 31 cycles in a programmable thermal cycler (Eppendorf AG, Hamburg, Germany). The program used was: 94ºC for 5 min and cycles of 94ºC for 15 s, 60ºC for 30 s, 72ºC for 40 s, with a final extension at 72ºC for 5 min. PCR products were analyzed by electrophoresis in 1% agarose gels. Once identified, genotyped animals were used as breeders for colony expansion and their offspring were used in all experimental procedures in which mice were required.

Behavioral studies

Female and male WT or TRESK KO mice between 8 and 15 weeks of age were used in all behavioral studies. To avoid stress-induced variability in the results, mice were habituated to the experimental room and the experimental setup prior to testing. Behavioral measurements were done in a quiet room, taking great care to minimize or avoid discomfort of the animals. All experimenters were blind to the genotype or the drug/vehicle assayed.

Mouse mechanical sensitivity

Mechanical sensitivity of WT and TRESK KO mice was assessed using the ‘up and down’ method by the application of calibrated von Frey filaments (North Coast Medical, Inc. Morgan Hill, CA) as previously described (Tulleuda *et al.*, 2011; Castellanos *et al.*, 2018). The von Frey filaments [size: 2.44, 2.83, 3.22,

3.61, 3.84, 4.08, 4.17, 4.31, 4.56; equivalent to (in grams) 0.04, 0.07, 0.16, 0.4, 0.6, 1, 1.4, 2 and 4] were applied perpendicularly to the plantar surface of the hind paw and gently pushed to the bending point for 5 s. The 50% withdrawal threshold was determined using the up and down method (Chaplan *et al.*, 1994). A brisk hind paw lift in response to von Frey filament stimulation was regarded as a withdrawal response. Dynamic plantar aesthesiometer (Ugo Basile, Italy) was also used to assess mechanical sensitivity. A von Frey-type 0.5 mm filament was applied with a 10 s ramp (0 to 7.5 g) and the hind paw withdrawal threshold of mice was recorded.

Mouse thermal sensitivity

Hot plate and cold plate test

After habituation, the cold/hot plate apparatus (Ugo Basile, Italy) was set to 2ºC, 52ºC or 56ºC and animals were individually placed in the center of the plate. Latency time to elicit a nocifensive behavior (a jump or a paw lick/lift) was counted with the apparatus stopwatch and the average of three separate trials was used as a measurement. Since the temperatures tested are in the noxious range, a cut-off time of 25 seconds was established to avoid tissue damage.

Dynamic hot plate test

In contrast to the conventional hot plate, the dynamic hot plate allows the testing of a wide range of temperatures. Before testing, animals were habituated and later placed individually to the hot/cold plate apparatus where the plate temperature increased from 30ºC to 50ºC at a 1ºC/min rate. To determine the temperature that is perceived as noxious for mice and quantify

pain-related behaviors, the number of jumps at each temperature was scored.

Radiant heat test

The heat sensitivity of mice was assessed by measuring hind paw withdrawal latency from a radiant infrared source (Hargreaves' method) using the Ugo Basile (Italy) Model 37370 Plantar test. Each measurement was the mean of 3 trials spaced 15 min apart. For all experiments, infrared intensity was set to 30% and a cut-off time of 20 seconds was established to avoid skin burn damage.

Thermal place preference test

The thermal place preference test is a test of better comfort temperature rather than an indicator of temperature aversion. The hot/cold plate apparatus was placed side by side with a complementary plate and a small divider platform was situated between them to connect the two devices (Ugo Basile, Italy). The reference plate was always set at 30ºC and the test plate was set at 50, 40, 30, 20, 15 or 10ºC. Animals were habituated at the experience room for 30 minutes before testing and then they were allowed to investigate the testing setup for 10 minutes or until animals crossed consistently from one plate to the other. Mice were then placed individually onto the center of the platform and once they crossed to a plate the cumulative time they spent on each plate for a total of 5 minutes was then counted. Only animals that performed properly when both plates were set to 30ºC were used for the study (50% of the time at each plate and more than 2 crossings). To exclude the possibility that animals could be learning which one the reference plate was, the position of the reference and

the test plate was switched randomly between trials.

Cold plantar assay

To complement the cold plate test, we studied noxious cold sensitivity of TRESK KO mice using the cold plantar assay (Brenner *et al.*, 2012). This assay produces an unambiguous nocifensive response that is easily identified when compared to the cold plate test. Animals were placed on top of a 1/8'' thick glass plate and were enclosed in transparent boxes separated by opaque dividers to prevent animals to see each other. The cold probe consisted of a modified 3 mL syringe filled with freshly powdered dry ice. This powder was then packed into a pellet and its surface was flattened. Using a mirror to target the mouse hind paw, we applied the dry ice pellet below the glass, making sure that the paw was completely in contact with it. This delivers a cooling ramp to the mice paw and a few seconds later withdrawal responses occur. The withdrawal latency time was measured with a stopwatch and the final withdrawal latency time for each animal was the average of 3 trials, which were tested at intervals of at least 15 minutes. A cut-off time of 20 seconds was used to prevent tissue damage.

Evaluation of nocifensive behavior

Using a 30g needle, 10 µl of a solution containing 100 µM AITC (10%), capsaicin (1µg/10µl) or their vehicle solutions were administered intradermally into the plantar surface of the hind paw. Mice behavior was observed and the number of flinches and lickings of the paw were counted for a 5-minute period

starting immediately after the injection. On the day previous to testing, animals were habituated to the testing room and to the handling procedure. The flinching and licking test was also used to examine the painful response of mice to different osmolality solutions, both in naive and sensitized conditions. 10 µl of the following solutions were administered in the hind paw to different groups of male mice: NaCl -33% (hypotonic, 100 mOsm·Kg^{-1}), NaCl 2% (hypertonic, 622 mOsm·Kg^{-1}), NaCl 10% (hypertonic, 3157 mOsm·Kg^{-1}) and PBS (Isotonic, 298 mOsm·Kg^{-1}). A different group of animals was used to study osmotic pain under inflammatory conditions. A 5 µl injection of prostaglandin E_2 (PGE_2; 10 µM) was injected into the hind paw of each mouse and 30 minutes after, 10 µl of NaCl -33% or NaCl 2% were injected into the sensitized paw. After the injection of different osmolality solutions, nocifensive behaviors of paw licking and shaking were manually counted for 5 minutes.

CFA model of inflammatory pain

After baseline measurements and under brief isoflurane anesthesia, Complete Freund's Adjuvant (CFA, Sigma-Aldrich; 20 µl; 1mg/ml) was injected subcutaneously (glabrous skin) in the hind paw of mice to induce a local inflammation. Mechanical von Frey threshold and heat withdrawal latency (radiant heat test) was examined at different time points after the injection (1h, 5h, 1d, 3d, 7d and 16d).

Formalin test

After habituation, mouse hind paw was subcutaneously injected with formalin (10 µl of a 5% formaldehyde solution) and nocifensive behaviors were

measured for 50 minutes after the injection. The cumulative time spent shaking and licking the injected paw was counted with a stopwatch in 5 min periods.

Oxaliplatin-induced cold hypersensitivity

Prior to oxaliplatin injection, naive thermal preference was measured with the thermal place preference test set at 20ºC vs. 30ºC. Thirty min later, paw withdrawal latency to cold stimuli was determined using the cold plantar assay. A single intraperiotoneal injection of oxaliplatin (6 mg/Kg in PBS with 5% glucose) was delivered to mice. Cold preference and cold sensitivity were re-evaluated 90 h after oxaliplatin injection, a time point that is known to correlate with the peak of oxaliplatin-induced cold hyperalgesia (Descoeur *et al.*, 2011).

Cuff-induced neuropathic pain model

The sciatic nerve cuffing model was used to induce mechanical and thermal hyperalgesia in the hind paw of mice, as described in (Yalcin *et al.*, 2014). Mice were housed individually to avoid stress derived from the surgery and to prevent injury. Cardboard rolls were placed into their home cages to provide shelter and additional stimulation after the surgery. All surgeries were done under aseptic conditions using intraperitoneal ketamine/xylazyne anesthesia. The left leg of mice was shaved from the hip to the knee and the surgical field was disinfected. A 0.5 cm incision parallel to the femur was made to expose the common branch of the sciatic nerve, which appeared after separating the muscles close to the femur. A drop of sterile physiological saline was applied to prevent the nerve from dehydrating and this concluded the procedure for the sham group. The ‘cuff’ consisted of a 2 mm-long piece of polyethylene tubing (PE-20) with an

inner diameter of 0.38 mm and an outer diameter of 1.09 mm, opened by one of its sides. For the cuff group, the sciatic nerve was gently straightened with two sterile sticks and the ‘cuff’ was inserted around the main branch of the nerve and closed by applying moderate pressure with surgical forceps. To ensure that the ‘cuff’ was correctly positioned and closed, it was turned gently around the nerve. Both sham and cuff surgeries ended by suturing the incision with surgical knots. After the procedure, animals were placed in their respective home cages lying on their right side and were under constant monitoring until they were completely awakened. Mechanical and heat sensitivity of mice were determined with the von Frey and the radiant heat tests as previously described, before surgery and 5, 7, 14 and 21 days after surgery.

Skin-nerve preparation and single fiber recordings

The isolated skin-saphenous nerve preparation for single C-fiber recording was used as previously described (Noël *et al.*, 2009). The hind paw skin of male mice 10 to 20 weeks of age was isolated with the saphenous nerve. The skin was pinned corium side up in a perfusion chamber with the nerve being pulled in a recording chamber filled with paraffin oil. The skin was perfused with warm (~30-31°C) synthetic interstitial fluid (SIF), in mM: 120 NaCl, 3.5 KCl, 5 $NaHCO_3$, 1.7 NaH_2PO_4, 2 $CaCl_2$, 0.7 $MgSO_4$, 9.5 Na-Gluconate, 5.5 glucose, 7.5 sucrose, and 10 HEPES, pH 7.4 adjusted with NaOH, saturated with O_2/CO_2 95%/5%. Isolated nerve fibers were placed on a gold recording electrode connected to a DAM-80 AC differential amplifier (WPI), Digidata 1322A (Axon Instruments) and Spike2 software (CED) to record extracellular potentials. The skin was probed with mechanical stimulation with a glass rod and calibrated von Frey filaments

to characterize the mechanical sensitivity of nerve fibers. The C-fibers were classified according to their conduction velocity of less than 1.2 m/s measured by electrical stimulation (Stimulus Isolator A385, WPI). The skin receptive field of C-fibers was isolated from the surrounding bath chamber with a stainless steel ring 0.8 cm in diameter, an internal volume of 400 µl, and a hot or cold temperature-controlled SIF was infused into the ring through a bipolar temperature controller CL-100 (Warner instrument). Electrical recordings were amplified (x10 000), band-pass filtered between 10 Hz and 10 kHz and stored on computer at 20 kHz. The action potentials were detected and analyzed offline with the principal component analysis extension of the Spike2 software (CED).

RNA extraction and Quantitative real-time PCR

Mouse tissue samples were obtained from dorsal root ganglia, kept in RNAlater solution (Ambion) and stored at -80ºC until use. Total RNA was isolated using the Nucleospin RNA (Macherey-Nagel) and first-strand cDNA was then transcribed using the SuperScript IV Reverse Transcriptase (Invitrogen, ThermoFisher Scientific) according to the manufacturer's instructions. Quantitative real-time PCR was performed in an ABI Prism 7300 using the Fast SYBR Green Master mix (Applied Biosystems) and primers (detailed below) obtained from Invitrogen (ThermoFisher Scientific). Amplification of Glyceraldehyde 3-phosphate dehydrogenase (GAPDH) transcripts was used as a standard for normalization of all qPCR experiments and gene-fold expression was assessed using the ΔC_T method. All reactions were performed in triplicate. After amplification, melting curves were obtained and evaluated to confirm

correct transcript amplification. Gene-specific primers used were: TRESK (forward 5′-CTCTCTTCTCCGCTGTCGAG-3′; reverse 5′-AAGAGAGCGCTCAGGAAGG-3′); TREK-1 (forward 5′-CACTGTGAGTTTTGCACATGG-3′; reverse 5′-GGGACTGGACTTTTTCTGAATC-3′); TREK-2 (forward 5′-GCAGCTTTCCCTTAGACCAG-3′; reverse 5′-CCAGGGACATTCATTTTGGA-3′); TRAAK (forward 5′-CATCCAAAAAGCCTTCCAGA-3′; reverse 5′-ATTTGGCAACCACTGGACTC-3′); TRPA1 (forward 5′-GCAGGTGGAACTTCATACCAACT-3′; reverse 5′-CACTTTGCGTAAGTACCAGAGTGG-3′); TRPV1 (forward 5′-CCCATTGTGCAGATTGAGCAT-3′; reverse 5′-TTCCTGCAGAAGAGCAAGAAGC-3′); GAPDH (forward 5′-ATGTGTCCGTCGTGGATCTGA-3′; reverse 5′-GCTGTTGAAGTCGCAGGAGAC-3′).

Culture of dorsal root ganglion neurons

Mice were euthanized by decapitation under anesthesia (isoflurane) and thoracic, lumbar and cervical dorsal root ganglia (DRG) were removed for neuronal culture as previously described (Tulleuda *et al.*, 2011; Callejo *et al.*, 2013). Briefly, DRGs were collected and maintained in cold (4–5°C) Ca^{2+} - and Mg^{2+} -free Phosphate Buffered Saline solution (PBS) supplemented with 10 mM glucose, 10 mM Hepes, 100 U.I./mL penicillin and 100 µg/mL streptomycin until dissociation. Subsequently, ganglia were incubated in 2 ml HAM F-12 with collagenase CLS I (1 mg/ml; Biochrome AG, Berlin) and Bovine Serum Albumin

(BSA, 1 mg/ml) for 1 h 45 min at 37ºC followed by 15 min trypsin treatment (0.25%). Ganglia were then resuspended in Dulbecco's Modified Eagle medium (DMEM) supplemented with 10% FBS, penicillin/streptomycin (100 µg/ml) and L-glutamine (100 mg/ml) and mechanical dissociation was conducted with fire-polished glass Pasteur pipettes of decreasing diameters. Neurons were centrifuged at 1000 rpm for 5 min and re-suspended in culture medium [DMEM + 10% FBS, 100 µg/ml penicillin/streptomycin, 100 mg/mL L-glutamine]. Cell suspensions were transferred to 12 mm-diameter glass coverslips pre-treated with poly-L-lysine/laminin and incubated at 37°C in humidified 5% CO_2 atmosphere for up to 1 day, before being used for patch-clamp electrophysiological recordings or calcium imaging experiments. Nerve Growth Factor or other growth factors were not added.

Calcium imaging

Cultured DRG neurons from wild-type and TRESK KO mice were loaded with 5 µM fura-2/AM (Invitrogen, Carlsbad, CA) for 45-60 min at 37ºC in culture medium. Coverslips with fura-2 loaded cells were transferred into an open flow chamber (0.5 ml) mounted on the stage of an inverted Olympus IX70 microscope equipped with a TILL monochromator as a source of illumination. Pictures were acquired with an attached cooled CCD camera (Orca II-ER, Hamamatsu Photonics, Japan) and stored and analyzed on a PC computer using Aquacosmos software (Hamamatsu Photonics, Shizuoka, Japan). After a stabilization period, pairs of images were obtained every 4 s at excitation wavelengths of 340 (λ1) or 380 nm (λ2; 10 nm bandwidth filters) in order to

excite the Ca^{2+} bound or Ca^{2+} free forms of the fura-2 dye, respectively. The emission wavelength was 510 nm (12-nm bandwidth filter). Typically, 20-40 cells were present in the microscope field. $[Ca^{2+}]_i$ values were calculated and analyzed individually for each single cell from the 340- to 380-nm fluorescence ratios at each time point. Only neurons that produced a response >10% of the baseline value and that, at the end of the experiment, produced a Ca^{2+} response to KCl-induced depolarization (50 mM) were included in the analysis. Several experiments with cells from different primary cultures and different animals were used in all the groups assayed. The extracellular (bath) solution used was 140 mM NaCl, 4.3 mM KCl, 1.3 mM $CaCl_2$, 1 mM $MgCl_2$, 10 mM glucose, 10 mM HEPES, at pH 7.4 with NaOH. Experiments were performed at room temperature.

Electrophysiological recording

Electrophysiological recordings in DRG sensory neurons were performed as previously described (Callejo *et al.*, 2013; 2015; Castellanos *et al.*, 2018). Briefly, recordings were performed with a patch-clamp amplifier (Axopatch 200B, Molecular Devices, Union City, CA) and restricted to small size DRG neurons (<30 μm soma diameter), which largely correspond to nociceptive neurons (Le Pichon & Chesler, 2014). Patch electrodes were fabricated in a Flaming/Brown micropipette puller P-97 (Sutter instruments, Novato, CA). Electrodes had a resistance between 2-4 MΩ when filled with intracellular solution (in mM): 140 KCl, 2.1 $CaCl_2$, 2.5 $MgCl_2$, 5 EGTA, 10 HEPES, 2 ATP at pH 7.3. Bath solution (in mM): 145 NaCl, 5 KCl, 2 $CaCl_2$, 2 $MgCl_2$, 10 HEPES, 5 glucose at pH 7.4. The osmolality of the isotonic solution was 310.6±1.8 mOsm/Kg. Membrane

currents were recorded in the whole-cell patch-clamp configuration, filtered at 2 kHz, digitized at 10 kHz and acquired with pClamp 10 software. Data was analyzed with Clampfit 10 (Molecular Devices) and Prism 7 (GraphPad Software, Inc., La Jolla, CA). Series resistance was always kept below 15 MΩ and compensated at 70-80%. All recordings were done at room temperature (22-23ºC), 18-24h after dissociation. To study sensory neuron excitability, after achieving the whole-cell configuration in the patch clamp technique, the amplifier was switched to current-clamp bridge mode. Only neurons with a resting membrane voltage below -50 mV were considered for the study. To study neuronal excitability, we examined the resting membrane potential (RMP); action potential (AP) rheobase (minimum current to elicit an AP; obtained with 400 ms depolarizing current pulses in 10 pA increments); whole-cell input resistance (R_{in}) was calculated on the basis of the steady-state I-V relationship during a series of 400 ms hyperpolarizing currents delivered in steps of 10 pA from -50 to -10 pA; AP amplitude was measured from RMP to AP peak, AP duration was measured at 50% of AP amplitude and hyperpolarizing afterpotential (HAP) was measured as the voltage difference between the firing level of the spike (beginning of the ascending phase of the action potential) and the potential of the HAP. The interspike interval was measured from peak to peak of two succeeding action potentials. The average of the initial three interspike intervals from spikes elicited by a 1s current ramp from 0 to 500 pA was used (Fig 2C).

Drugs

All reagents and culture media were obtained from Sigma-Aldrich (Madrid, Spain) unless otherwise indicated. Menthol (100 μM), allyl isothiocyanate (AITC; 100 μM) and capsaicin (1 μM) were also purchased from Sigma (Madrid, Spain).

Data analysis

Data are presented as mean ± SD or, in some specific analysis, the median, the coefficient of variation or the geometric mean is also provided. Statistical differences between different sets of data were assessed by performing paired or unpaired Student's t-tests, Mann-Whitney test, Wilcoxon matched pairs test, one-way or two-way ANOVA plus the Holm-Sidak correction for multiple comparisons, Chi-square test or Fisher's exact test, as indicated. The significance level was set at $p<0.05$ in all statistical analyses. Data analysis was performed using GraphPad Prism 8 software and GraphPad QuickCalcs online tools (GraphPad Software, Inc., La Jolla, CA)

Results

TRESK deletion reduces total background current and enhances neuronal excitability

TRESK channels have been detected in small- and medium-sized sensory neurons, together with other members of the K_{2P} family of background K^+ channels (Kang & Kim, 2006; Usoskin *et al.*, 2015; Zeisel *et al.*, 2018). To confirm the loss of TRESK expression in homozygous knockout animals and to assess possible compensatory effects on the expression of other K_{2P} channels, we examined the mRNA expression in DRGs by real-time quantitative PCR. TRESK mRNA was undetected in KO mice while a significant expression was found in wild-type (WT) animals (Fig 1A). We next examined the expression of TREK-1, TREK-2 and TRAAK (the most expressed K_{2P}s in sensory neurons). Analogously to what has been reported in a previous study (Chae *et al.*, 2010), mRNA for these channels were present in WT and KO mice at similar levels, thus excluding any compensation effect. Furthermore, the expression of TRPA1 and TRPV1, two channels highly expressed in nociceptors, was also unchanged.

To assess whether removal of TRESK modifies K^+ background currents in nociceptors, we recorded total K^+ current from small diameter DRG neurons (soma size <30 μm; capacitance <45pF) that largely correspond to nociceptive neurons with C-fiber conduction velocities (Ma *et al.*, 2003).

Putative nociceptors isolated from KO mice displayed a significantly smaller K^+ current density than nociceptors of WT mice, both at -25 mV (15.3±8.5; n=31; vs. 9.7±7.8 pA/pF; n=50; for WT and KO mice, respectively; unpaired t-test p=0.004), and -135 mV (-11.1±8.9 pA/pF vs. -7.3±5.6 pA/pF; for WT and KO mice, respectively; unpaired t-test p=0.038), indicating that the absence of TRESK has a significant functional consequence on the membrane current (Fig 1B). In a second set of nociceptor recordings, we investigated the functional consequence of TRESK deletion on neuronal excitability by measuring their resting membrane potential and action potential firing properties (Fig 2A and B). Wild-type and TRESK KO nociceptors did not present significant changes in resting membrane potential (RMP: -58.3±13.6 vs. -56.2±7.7 mV, respectively. Unpaired t-test p=0.540; Fig 2B), suggesting that TRESK might have a minor role in setting the RMP and other K^+ channels are possibly more important in setting the RMP in the cell body. This is in agreement with previous data where RMP was not significantly modified after TRESK down-regulation or deletion (Dobler *et al.*, 2007; Tulleuda *et al.*, 2011). Interestingly, current-clamp recordings indicated that rheobase (minimum current injected to elicit an action potential) was significantly lower in TRESK KO nociceptors (Fig 2B, p=0.0013 unpaired t-test) compared to nociceptors from WT littermates. This effect is likely a consequence of the increased membrane resistance found in TRESK KO neurons (1262.8±655.3MΩ) compared to controls (WT: 792.7±661.7MΩ; p=0.045 unpaired t-test; Fig 2B). As expected, action potential amplitude was not significantly altered (p=0.406, unpaired t-test) since this parameter is more dependent on the activity of voltage-dependent sodium channels (Na_V). However, action potentials were significantly wider in nociceptors from TRESK

KO, likely reflecting the consequence of the decrease in total K^+ current (width at 50% AP: TRESK KO 4.03±2.4 ms; n=27 neurons; Wild-type: 2.38±1.9 ms; n=13; p=0.041; Fig 2B). In a similar fashion, hyperpolarizing afterpotential (HAP) measured from the firing level of the spike was also reduced in KO neurons (TRESK KO 36.5±7.7 mV; n=27 neurons; Wild-type: 46.4±8.1 mV; n=13; p=0.001). To investigate if these changes affect the excitability of nociceptors, we injected a depolarizing current ramp (0 to 500 pA, 1s) and counted the number of action potentials generated for each genotype. As shown in Fig 2C, TRESK KO neurons fired on average more spikes (13.6±5.4 spikes; n=18) than WT neurons (8.3±5.8 spikes; n=10; p=0.023), and showed a reduced interspike interval (KO: 70.6±23.9 ms *vs*. WT: 111.2±54.7 ms; p=0.006), indicating that removal of TRESK increased the excitability of sensory neurons.

To further characterize the responsiveness of sensory neurons in TRESK KO mice, we measured the intracellular Ca^{2+} signals ($[Ca^{2+}]$) of cultured DRG neurons from WT and KO mice in response to capsaicin (1 μM; TRPV1 agonist) and AITC (100 μM; TRPA1 agonist), two markers of nociceptive neurons, and menthol (100 μM; TRPM8 agonist), a marker of cold sensory neurons. Among WT sensory neurons (total number of neurons analyzed = 1124), 49.2% responded to capsaicin, 40.4% to AITC and 7.0% to menthol. Responses to both capsaicin and AITC were seen in 17.9% of the neurons (Fig 3A and B). A percentage of neurons did not respond to any of the agonists tested (246 neurons, 21.9%). Responses to capsaicin (45.7%) and menthol (9.1%) were not different in neurons from TRESK KO mice (n=1228) but, the percentage of

neurons activated by AITC was significantly lower (24.7%, p=0.009). Neurons non-responding to any agonists were 446 (36.3%). The diameters of sensory neurons responding to the different agonists between WT and KO animals were not different, indicating that they represent similar populations of DRG neurons (mean soma diameter WT: 20.2±5.9 µm; KO: 20.3±5.6 µm). In parallel experiments, the response of cultured trigeminal neurons was assessed. These showed no significant differences for the response to the different agonists (data not shown) between genotypes. Therefore, the diminished response to AITC is restricted to DRG neurons.

We next assessed if the reduced AITC response of DRG neurons from TRESK KO mice had a behavioral correlate by injecting AITC (100 µM) into the mouse hind paw. In agreement with the decreased response to AITC obtained in calcium recordings, nocifensive behavior measured as the time spent licking or shaking the paw significantly diminished in KO compared to WT mice (TRESK KO: 9.0±7.3 s; WT: 18.1±13.0 s; p=0.039; n=13 for each group; Fig 3C). In contrast, painful behavioral responses to capsaicin injection did not differ between KO and WT mice (40.0±22.7s vs. 28.8±13.6s, respectively; p=0.236; Fig 3C). Injection of vehicles for each compound did not produce significant behavioral effects (data not shown). To further investigate to what extend chemical nociception was altered by the absence of TRESK, we used the formalin test (Tjølsen *et al.*, 1992; Abbott *et al.*, 1995), which is characterized by an initial phase (phase I; 0-5 min) due to direct nociceptor activation (McNamara *et al.*, 2007) and a second phase (phase II; 15-50 min) that is attributed to a combined nociceptive input together with central spinal

sensitization (Tjølsen *et al.*, 1992). The phase I nocifensive response has been directly linked to the activation of TRPA1 (McNamara *et al.*, 2007) although high concentrations of formalin are still able to induce some pain in TRPA1 KO mice (Fischer *et al.*, 2013). Interestingly, animals lacking TRESK showed a diminished response to a 5% formalin injection in phase I (30.8±15.0 s; p=0.002; Fig 3D) compared to control WT animals (69.9±17.6s). The decreased response in phase I of TRESK KO animals is in agreement with the decreased nocifensive response observed after AITC injection (Fig 3C) which corroborates the decreased fraction of AITC sensitive DRG neurons from TRESK KO in culture. All these observations confirm that TRPA1 activation is decreased in TRESK KO animals. Phase II of the formalin test can be further split in phase IIa (15-25 min) and IIb (25-50 min), where IIa has a higher nociceptive input than IIb. TRESK KO animals showed a decreased licking time during phase IIa (107.7±39.9s) compared to wild-type animals (154.8±42.2s; p=0.026); which probably reflects a decreased nociceptors activation as found in phase I. In contrast, phase IIb of the formalin test did not show significant differences and licking behavior was similar between groups (p=0.814, Fig 3D). Injection of hypertonic saline stimulates primary afferent nociceptors and produce pain in humans (Alessandri-Haber *et al.*, 2003; 2005). This response can be further enhanced by sensitization of nociceptors with PGE_2. Injection of hypotonic stimuli did not induce significant nocifensive behavior in resting conditions (p=0.146, Fig 3E) but, as previously described (Alessandri-Haber *et al.*, 2003; Alloui *et al.*, 2006), nocifensive responses were enhanced after sensitization with PGE_2 in WT mice but not in TRESK KO mice (p=0.019, unpaired t-test WT vs. KO). Nocifensive responses to mild hypertonic saline were diminished in

TRESK KO animals both, in resting conditions (2% or 10% NaCl, p=0.049 and p=0.002) or after sensitization with PGE_2 (p=0.002; Fig 3E). Again, these effects are similar to the one reported after knocking out TREK-1 and TREK-2, but not in the single TRAAK knockout mice (Alloui *et al.*, 2006; Noël *et al.*, 2009; Pereira *et al.*, 2014), thus implying that TREK-1, TREK-2 and TRESK are involved in the sensitivity to hypertonic stimuli and their absence prevents sensitization by PGE_2.

Mice lacking TRESK present mechanical allodynia and normal heat perception

Since TRESK knockout enhances nociceptor excitability, we next analyzed the sensitivity of nerve fibers from TRESK KO mice to different types of stimuli and whether the activation of sensory fibers was correlated to behavioral responses to these stimuli. Saphenous nerve C-fibers from WT (n=14) and TRESK KO mice (n=22) were recorded with the nerve-skin preparation (Zimmermann *et al.*, 2009). Mechanical thresholds were determined with calibrated von Frey filaments applied on the receptive fields of C-fibers. TRESK KO mice presented an enhanced sensitivity to mechanical stimuli. Mean threshold value for the whole population was not significantly different in KO animals (mean±SD: 27.6±24.6 mN; median: 22 mN) compared to WT mice (mean±SD: 33.2±23.3 mN; median: 22 mN; p=0.268, Mann-Whitney test), but threshold values from KO mice presented a wider distribution and a significant shift towards lower values (Fig 4A). This wider spread might mean a subset of C-fibers have lost the inhibitory effect of TRESK, and can now activate with lower-intensity mechanical stimuli. To examine such possibility, we compared percentage of

fibers that presented a lower threshold for activation by mechanical stimuli. Our results indicate that KO mice presented a significant percentage of fibers with lower thresholds (<12 mN; 40.9%) compared to fibers from WT animals (0%; p=0.006; Fisher's exact test). This wider distribution of mechanical thresholds towards lower values in the fibers from KO animals can be also shown by the larger coefficient of variation (WT: 70.2% vs. KO: 89.1%) and by the geometric mean (WT: 27.8 mN vs. KO: 17.6 mN; Fig 4A, blue lines), which normalizes the ranges being averaged, thus no range dominates the weighting. This suggests that TRESK function prevents C-fiber activation by low intensity mechanical stimuli and therefore deletion of the channel reveals mechanical sensitivity with low threshold values in a fraction of C-fibers (Fig 4A). We then compared the mechanical sensitivity of TRESK KO to WT mice with the von Frey up and down method. Hind paw mechanical threshold was significantly lower in TRESK KO mice compared to WT ($p<0.0001$ for males and females; Fig 4B), thus indicating that the subset of C-fibers with lower activation thresholds by mechanical stimuli have an important functional consequence since they precipitate mechanical allodynia in awake, freely-moving mice. Measures of mechanical sensitivity with the dynamic plantar aesthesiometer also confirmed significant differences to pressure application between WT (5.06 ± 0.61 g; n=27) and KO animals (4.66 ± 0.81 g; n=22; t-test p=0.027; Fig 4B).

Although other members of the K_{2P} family have been involved in thermosensation and pain perception in response to hot or cold stimuli (Alloui *et al.*, 2006; Noël *et al.*, 2009; Pereira *et al.*, 2014), TRESK activity is not modulated by changes in temperature in the physiological range (Kang & Kim,

2006). Despite this lack of thermal sensitivity of the channel, it remains possible that the channel modulates the excitability of C-fibers involved in heat sensitivity. We addressed this question by recording responses of C-fibers activated by a heat-ramp applied on their receptive fields in the skin. TRESK KO and WT mice did not show significant differences in heat thresholds for the activation of C-fibers (37.6±2.8ºC, n=35 C-fibers for WT; 38.1±3.9ºC, n=37 C-fibers for KO; p=0.502 t-test; Fig 4C), nor the distribution of these thresholds in a range of temperatures, nor the number of spikes fired by heat sensitive C-fibers during heat-ramps (32.6±28.2 spikes WT; 34.8±28.3 spikes TRESK KO; p=0.720 t-test; Fig 4C), indicating that TRESK does not seem to have a major role in the detection of warm or hot temperatures. We then tested heat sensitivity *in vivo* using the Hargreaves' and hot plate tests. Heat sensitivity was unaltered in TRESK KO mice compared to WT in the radiant heat Hargreaves test (p=0.08 males; p=0.603 females, Fig 4D), thus confirming the observations made in C-fibers recordings. To further evaluate a possible implication of TRESK in heat pain, we evaluated the sensitivity to more extreme temperatures in the hot plate test at 52 and 56ºC, but no significant differences were detected (Fig 4D). This indicates that the extreme heat sensitivity is conserved in TRESK KO mice. The dynamic hot plate with a ramp of temperature has been proposed as a valuable method to differentiate between thermal allodynia and hyperalgesia (Yalcin *et al.*, 2009). The number of jumps of the mice on a hot plate when the plate temperature is increased from 39 to 50 ºC did not show any difference between TRESK KO and WT, neither for the total number of jumps nor the temperature at which animals displayed their first jump (Fig 4E). These behavior and skin-

nerve preparation results indicate that there is no significant contribution of TRESK to heat sensitivity.

Elevated perception of cold temperatures in the absence of TRESK channel

Thermosensitivity to cold temperatures is governed by different mechanisms and by distinct neuronal subpopulations than warm/hot perception (Lolignier *et al.*, 2016). We evaluated the role of TRESK in the cold sensitivity of C-fibers by recording fibers activity with the saphenous nerve preparation upon cooling their receptive fields in the skin from 30 to 10ºC over 90 s (Fig 5A-D). C-fiber recordings from TRESK KO mice showed that although the total number of cold-sensitive fibers did not differ significantly (58% in WT and 66% in KO mice), there were significant changes in the fractions of mechano-cold and mechano-heat and cold sensitive polymodal C-fibers compared to WT mice. Specifically, we observed in KO mice an increase in the fraction of mechano-cold C-fibres compared to WT mice (37% vs. 20% C-MC, respectively; Fig 5A). This was accompanied by a reduction of the percentage of mechano-heat-cold C-fibers (C-MHC) in KO mice (29%) compared to WT (38%; $p<0.01$; Chi-square test; Fig 5A). The distribution of C-fibers activation thresholds by cold stimuli indicated a clear shift toward warmer temperature in the KOs (between 26-28ºC) than in the WT (Fig 5B and 5C). Despite the mean or median cold thresholds not being different ($p=0.565$, Mann-Whitney test; Fig 5C), we observed a tendency to have more fibers activated at temperatures above 25ºC in KO animals (58%) compared to WT (42%), although this difference did not reach statistical significance (Fisher's exact test; $p=0.099$). The total response of TRESK KO

fibers to a 90 s cooling ramp (33.1±29.5 spikes) was similar to that of WT fibers (34.1±25.1 spikes; p=0.90 unpaired t-test). However, the distribution of the activity upon cooling was higher at temperatures between 25 and 19ºC in TRESK KO fibers (Fig 5D). The baseline activity between 30-31ºC was also higher in TRESK KO than WT fibers (0.3 spikes/s for TRESK KO and 0.1 spikes/s for WT; n=36 and n=31 respectively; p<0.001, t-test). These experiments indicate that the temperature for activation of cold-sensitive C-fibers was higher in TRESK KO, but also that the overall fiber activity in response to cooling did not depend drastically on the presence of TRESK.

In agreement with observations in C-fibers, behavioral responses to cold were also altered in animals lacking TRESK. Sensitivity to noxious cold (2ºC; cold plate test) was enhanced in knockout animals from both sexes, with shorter latency times to elicit a nocifensive behavior (p=0.006 males; p=0.041 females, Fig 5E). In addition, cold sensitivity to more moderate temperatures assessed with the cold plantar assay was significantly higher in TRESK KO mice (p<0.0001 males, p=0.008 females, Fig 5F). Finally, we assessed whether changes in cold sensitivity modified the preference the mice displayed between the two different temperatures. TRESK KO animals spent more time on the reference plate (at 30ºC) than on the experimental plate at 20ºC (p=0.015, one-way ANOVA plus Holm-Sidak correction for multiple comparisons, Fig 5G) compared to wild-type animals, further supporting previous evidence from cold sensitive C-fibers recordings and cold sensitivity assays. In contrast, place preference assays at other temperatures (10, 15, 30, 40, 50ºC) did not show significant alterations between mice genotypes, corroborating the non-

involvement of TRESK in the perception of cool, warmth or hot temperatures (Fig 4).

Mice lacking TRESK show selective changes in persistent inflammatory and neuropathic pain

To assess the contribution of TRESK in chronic pain conditions, the behavior of TRESK KO and WT mice was measured after intraplantar CFA injection, a model of persistent inflammatory pain. Both genotypes developed mechanical and thermal hypersensitivity in the injected hind paw beginning 1h after injection and lasting at least 16 days (Fig 6A). Despite the initial difference in basal mechanical thresholds ($p=0.047$), the extent of mechanical allodynia was similar between WT and KO animals 1h after CFA injection and during the entire 16 days observation period ($p>0.05$; two-way ANOVA plus Holm-Sidak correction for multiple comparisons). The development of thermal hyperalgesia was similar between both genotypes, thus showing that TRESK does not contribute significantly to peripheral sensitization of nociceptors due to inflammation. The sciatic nerve cuff-model was used to evaluate TRESK contribution in persistent neuropathic pain. Mechanical hypersensitivity developed in KO animals was significantly higher to begin with ($p=0.0006$; Fig 6B) but no significant differences were found after sciatic nerve cuffing compared to WT animals. Sham surgery did not show significant effects on this parameter in any genotype compared to baseline values (Fig 6B). Also, when the percent change in threshold (difference vs. basal value) was compared between WT and KO animals, this showed similar values (at 5 days, KO: -45.1±42.7%; WT: -37.9±29.6%; $p=0.742$; at 7 days, KO: -47.3±41.5%; WT: -45.0±47.3%; $p=0.931$),

indicating that nerve injury exerted a similar effect in both genotypes but, since KO had a lower mechanical threshold to begin with, animals reached lower mechanical thresholds at days 5 and 7. Mechanical hypersensitivity was undistinguishable between groups at later stages, at 14 and 21days post-injury. Heat sensitivity showed a similar level of hyperalgesia after neuropathy, akin to the lack of implication of TRESK in thermal perception. Surprisingly, withdrawal latencies from KO animals recovered to baseline values faster than WT group after 21 days, which could indicate an excitotoxic death of some of the primary afferents due to excessive hyperactivity. Finally, we evaluated chemotherapy-induced neuropathic pain with the anti-cancer drug oxaliplatin, which induces cold allodynia in a majority of patients. To assess whether the development of cold hyperalgesia after oxaliplatin treatment was modified in TRESK KO. As expected, wild-type mice showed an enhanced cold sensitivity 90h after the oxaliplatin injection. Both, cold plantar assay ($p=0.0002$; paired t-test) and thermal place preference test (30/20ºC; $p=0.0045$; unpaired t-test) showed significant differences compared to pre-injection values, indicating a higher sensitivity to cold stimuli in neuropathic mice (Fig 6C). In contrast, when TRESK KO animals were tested in the cold plantar assay, we did not observe any further decrease in paw withdrawal latency compared to the baseline value ($p=0.912$), which was already lower than that of WT animals. Again, thermal place preference between 20 and 30ºC did not show significant differences after oxaliplatin treatment ($p=0.770$), suggesting that the enhanced cold sensitivity due to TRESK removal cannot be further increased by neuropathy induced by oxaliplatin.

Discussion

TRESK is highly expressed in sensory ganglia (Kang & Kim, 2006; Dobler *et al.*, 2007; Bautista *et al.*, 2008; Tulleuda *et al.*, 2011; Manteniotis *et al.*, 2013; Nguyen *et al.*, 2017; LaPaglia *et al.*, 2018; Ray *et al.*, 2018) within specific subtypes of sensory neurons, mainly nociceptors and especially in non-peptidergic ones (Chiu *et al.*, 2014; Usoskin *et al.*, 2015; Li *et al.*, 2016; Nguyen *et al.*, 2017; Zheng *et al.*, 2019). TRESK main role has been attributed to preventing neuronal depolarization (Enyedi & Czirják, 2010), and reduction of its expression after nerve injury or inflammation contribute to neuronal hyperexcitability (Dobler *et al.*, 2007; Tulleuda *et al.*, 2011; Marsh *et al.*, 2012). Mutations in this channel have been linked to the enhanced nociceptor excitability that occurs during familial migraine with aura (Lafrenière *et al.*, 2010; Royal *et al.*, 2019). Here, we propose that TRESK balances the effects of depolarizing stimuli, acting as a brake to prevent the activation of specific subpopulations of sensory neurons.

Nociceptors lacking TRESK presented electrophysiological changes and an enhanced excitability consistent with its putative role to prevent neuronal depolarization (Kang & Kim, 2006). Resting membrane potential was similar between TRESK KO and WT neurons, indicating that TRESK does not contribute significantly in setting this parameter, as previously suggested (Dobler *et al.*, 2007). Indeed, other K_{2Ps} and other K^+ channel families have been proposed to control membrane polarization at rest (Du *et al.*, 2018). We found that TRESK, TREK-1 and TREK-2 were similarly expressed in DRGs, while the expression of TRAAK was lower. Others have found a slightly higher

expression of TRESK over TREK-1 or TREK-2 while the expression of TRAAK varies in different studies but in general appears less expressed than TRESK (Dobler *et al.*, 2007; Marsh *et al.*, 2012). Despite unchanged mRNA expression of other leak channels (TREK-1/2, TRAAK) in TRESK KO mice, it is possible that post-translational modifications of these proteins in TRESK KO mice exist, thus enhancing the functional contribution of these other K^+ currents in the absence of TRESK to maintain the membrane potential within the physiological range. Also, a compensatory effect by other channels (e.g. HCN, KCNQ) cannot be discarded. TRESK might have a major impact on the range between the resting membrane potential and the action potential threshold, thus effects observed in excitability appear to be mainly attributable to the specific removal of TRESK. Still, these effects could be underestimated by the fact that TRESK shows different levels of expression in different types of nociceptors (Usoskin *et al.*, 2015), thus studying specific subpopulations of genetically-labeled nociceptors (mainly non-peptidergic) might render larger effects in excitability after TRESK deletion. In fact, a recently published characterization in TG neurons shows that TRESK is present in 73% of $IB4^+$ non-peptidergic neurons, while only 29% of $CGRP^+$ neurons (mainly peptidergic nociceptors) express TRESK (Weir *et al.*, 2019). In agreement, $IB4^+$ nociceptive TG neurons showed an enhanced excitability compared to $IB4^-$ neurons. Another study have reported similar results in TG neurons but, surprisingly, lumbar DRG neurons from the same TRESK KO mice were not found hyperexcitable (Guo *et al.*, 2019). Despite we did not differentiate between $IB4^+$ and $IB4^-$ neurons in this study, our data supports previous findings of enhanced excitability of nociceptive sensory neurons (small-sized DRGs) either after TRESK deletion or

after a significant decrease in its expression (Dobler *et al.*, 2007; Tulleuda *et al.*, 2011; Yang *et al.*, 2018; Weir *et al.*, 2019). These effects have been also found after a decreased TRESK expression in a functional TRESK[G339R] knockout mice (Dobler *et al.*, 2007; Kollert *et al.*, 2015), after sciatic nerve axotomy (Tulleuda *et al.*, 2011) or in a model of cancer-associated pain (Yang *et al.*, 2018). This is in agreement with the neuronal activation observed by compounds blocking TRESK (Bautista *et al.*, 2008; Tulleuda *et al.*, 2011; Castellanos *et al.*, 2018) or with the decreased excitability when overexpressing the channel (Guo & Cao, 2014; Yang *et al.*, 2018), indicating that the regulation of TRESK expression is an important factor to control sensory neuron excitability.

Here, we found that instead of producing a general increase in excitability, removal of TRESK has a selective effect on certain types of fibers/sensory neuron subtypes affecting specific sensory modalities. In a similar fashion, genetic deletion of TREK-1 modifies mechanical, heat and cold pain perception (Alloui *et al.*, 2006) but when TRAAK is deleted, cold sensitivity remains unaffected and animals only present an enhanced heat sensitivity. Interestingly, deleting both channels (TREK-1/TRAAK double KO mice) potentiates the effects on cold sensitivity compared to TREK-1 alone (Noël *et al.*, 2009). Besides, deletion of TREK-2 only enhances thermal sensitivity to non-aversive warm temperatures but not to cold stimuli (Pereira *et al.*, 2014). Finally, eliminating the BK_{Ca} channel does not modify acute nociceptive or neuropathic pain, but enhances persistent inflammatory pain (Lu *et al.*, 2013), highlighting its specific participation during inflammation-induced hyperalgesia. Our data

suggests that the lack of TRESK enhances cold sensitivity by increasing the percentage of C-fibers activated at moderate cold temperatures, which is translated at the behavioral level by an enhanced sensitivity to cold stimuli. An increase in cold sensitivity has also been reported in the face of TRESK KO mouse using the acetone test (Guo *et al.*, 2019). In our study, the fraction of C-fibers activated by cold (C-MHC and C-MC; 58% in WT mice) was higher than other reports (between 35-45%), which could be due to the smaller number of fibers sampled compared to other studies (Bautista *et al.*, 2007; Noël *et al.*, 2009; Pereira *et al.*, 2014; Winter *et al.*, 2017) but, as occurred after deletion of other K_{2P} channels, the fraction of cold sensitive C-fibers was enhanced in TRESK KO mice compared to WT animals. Interestingly, the bigger fraction of cold sensitive C-MC fibers (37%) in KO animals compared to WTs (20%) suggests that, in physiological conditions, TRESK silences a population of neurons that would be normally activated at lower temperatures. This is consistent with a possible role of TRESK in preventing cold allodynia, acting as a brake to avoid C-fiber activation at moderate cool temperatures. In fact, knocking out TRESK mimics cold allodynia and oxaliplatin injection is not able to further increase cold sensitivity. Oxaliplatin-induced cold allodynia has been attributed to a combined remodeling of ion channels, including down-regulation of TREK-1, TREK-2, TRAAK, $K_v1.1$ and $K_v1.2$, coupled with up-regulation of TRPA1, $Na_v1.8$ and HCN1, while other channels (TRPM8) are not significantly modified (Descoeur *et al.*, 2011; Pereira *et al.*, 2014). It has been proposed that a reduced activity of K_{2P} channels when temperature decreases is responsible of releasing the excitability brake exerted by these channels and, combined with depolarizing thermo-TRP channels activation, triggers neuronal activation (Kang

& Kim, 2006; Noël *et al.*, 2009; Pereira *et al.*, 2014). This seems not to be the case for TRESK, since its activity (channel open probability) is not significantly modified by temperature between 20-37ºC (Kang & Kim, 2006). The possible modulation of the channel at lower temperatures it is unknown and remains to be tested.

TRPA1 was initially proposed to be involved in noxious cold sensing (Story *et al.*, 2003) but recent reports have questioned its role, hypothesizing that it might be regulating cold sensitivity indirectly, rather than acting as a cold-sensing receptor (Lolignier *et al.*, 2016; Yarmolinsky *et al.*, 2016; Winter *et al.*, 2017). If TRESK and TRPA1 are partially co-expressed in some neurons, one would expect an increase in the responses triggered by TRPA1 activation but, to our surprise, we observed the opposite effect despite TRPA1 mRNA expression is unchanged. It is possible that some other type functional regulation is present, but we did not explored this possibility further. Contrarily, it seems unlikely that enhanced cold sensitivity in TRESK KO animals is related to the observed decrease in TRPA1 activity. K_v channels can blunt cold responses by opposing to depolarizing stimuli in $TRPA1^+$ and $TRPM8^+$ neurons (Madrid *et al.*, 2009; Memon *et al.*, 2017). It is possible that TRESK might exert a similar effect, hence silencing cold responses in normal conditions. Therefore, releasing this excitability brake by knocking out or down-regulating TRESK expression enhances cold sensation. We did not found differences in the cellular responses to menthol, which activates TRPM8, a well-known sensor of cold temperatures (Bautista *et al.*, 2007). Also, TRESK and TRPM8 seem to be expressed in different subpopulations of sensory neurons (Usoskin *et al.*, 2015; Nguyen *et al.*,

2017) and the transcriptome of TRPM8^{+} sensory neurons does not show an appreciable TRESK expression (Morenilla-Palao *et al.*, 2014). Therefore, the enhanced cold sensitivity in TRESK KO mice does not seem related to activation of TRPM8^{+} fibers. Nevertheless, TRPM8^{+}/IB4^{-} trigeminal neurons have been reported to be more excitable in the TRESK KO compared with WT neurons (Guo *et al.*, 2019), thus an increase in activation of TRPM8^{+} fibers after TRESK deletion can not be completely discarded. Recently, a new cold sensor (GLR-3) has been identified in *C. elegans* and the kainate receptor GluK2 (mouse GLR-3 homolog) has been proposed to mediate cold sensitivity in mouse DRGs (Gong *et al.*, 2019). Whether this cold sensor is expressed in the same neurons that contain TRESK it is yet unknown. Even if this is the case, it remains to be examined in greater depth.

Mechanical sensitivity is also enhanced in TRESK KO animals, which present a higher number of C-fibers with lower mechanical thresholds and an increased response to von Frey hairs application. Similar results were previously reported after knocking down TRESK expression or after injecting TRESK blockers, where animals showed mechanical allodynia (Tulleuda *et al.*, 2011; Castellanos *et al.*, 2018; Yang *et al.*, 2018). Likewise, trigeminal expression of a mutated form of TRESK linked to migraine results in facial mechanical allodynia (Royal *et al.*, 2019). Other studies have also reported an increase in innocuous touch sensitivity in mice after TRESK deletion although they did not find a significant difference in punctate mechanical sensitivity (Weir *et al.*, 2019). A decrease in the withdrawal threshold to application of von Frey filaments in the forehead skin (trigeminal area) has also been reported but, surprisingly, not in the

hindpaw (Guo *et al.*, 2019). In our study, mechanical sensitivity is enhanced by shifting the mechanical threshold toward lower values in a population of sensory fibers, and therefore, a higher number of fibers is activated by low intensity mechanical stimulation. Piezo2 channel is involved in the detection of both innocuous touch and high threshold noxious mechanical stimuli due to its expression in low threshold mechanoreceptors (LTMR) and nociceptors (Ranade *et al.*, 2014; Dhandapani *et al.*, 2018; Murthy *et al.*, 2018; Szczot *et al.*, 2018), and has been proposed to play a crucial role in the generation of mechanical allodynia during inflammation and neuropathic pain (Murthy *et al.*, 2018). TRESK is also highly expressed in these populations of sensory neurons involved in mechanical hypersensitivity (Usoskin *et al.*, 2015). We can hypothesize that when these neuronal populations lack TRESK, they are more readily activated by mechanically activated currents coming through Piezo2 or other mechanosensitive channels such as the recently identified TACAN (Beaulieu-Laroche *et al.*, 2018), that would depolarize sensory neurons more effectively. We have not evaluated whether LTMR lacking TRESK are more excitable and if other touch modalities such as light touch (brush stroke) are also enhanced, but mechanical allodynia present in these animals suggests that they might also be affected. In agreement, a recent report found an enhanced response to innocuous touch stimuli (Weir *et al.*, 2019).

TRESK is notably expressed in MrgprD^{+} neurons (Usoskin *et al.*, 2015; Zheng *et al.*, 2019) and deletion of this subpopulation of neurons abolishes mechanical but not thermal pain (Cavanaugh *et al.*, 2009). Here, the mechanical hypersensitivity found after TRESK deletion might suggest an enhanced

excitability of MrgprD$^+$ neurons. In contrast, mechanical sensitization that occurs after inflammation or injury is not further enhanced by the absence of TRESK. Our data suggests that the molecular effect of injury, down-regulating TRESK expression (Tulleuda *et al.*, 2011), has already been achieved by genetic removal of TRESK, thus any further decrease in mechanical threshold observed is likely due to other mechanisms sensitizing nociceptors or derived from central effects.

TRESK KO mice did not display relevant differences in heat sensitivity. Only the thermal place preference between 20/30ºC showed a difference that seems to reflect the enhanced cold sensitivity rather than any effect on warm/heat sensitivity. In agreement, TRESK KO C-fibers did not show any specific effects upon temperature increase compared to WT. No significant alterations on heat sensitivity were either observed after CFA-induced inflammation or in the neuropathic pain model. In contrast to other K_{2P} and TRP channels (Alloui *et al.*, 2006; Noël *et al.*, 2009; Julius, 2013; Vriens *et al.*, 2014; Pereira *et al.*, 2014; Yarmolinsky *et al.*, 2016), the role of TRESK in neurons detecting warm or hot stimuli seems not to be highly relevant. Chemical sensitivity was altered for some stimuli (AITC, osmosensitivity) but not for others (capsaicin, menthol). Whether TRESK is directly involved in detecting osmotic stimuli is unlikely, although we previously described that hypertonic and hypotonic stimuli modulate TRESK currents (Callejo *et al.*, 2013). Similar results in osmotic pain were reported in animals lacking TREK or TRPV4 channels (Alessandri-Haber *et al.*, 2005; Alloui *et al.*, 2006; Noël *et al.*, 2009; Pereira *et al.*, 2014). Similarly to TREK-1/2 KO mice (but not TRAAK KO), PGE_2 was unable to sensitize

nociceptors to osmotic stimuli in TRESK KO animals. It has been proposed that the negative regulation of TREK-1/2 channels by cAMP/PKA downstream of the G-coupled PGE_2 receptor might be involved in the lack of PGE_2-mediated nociceptor sensitization. PKA is known to phosphorylate TRESK and keep it in a resting state where the channel is less active (Czirják & Enyedi, 2010) but a direct link between PKA activation, TRESK activity and osmotic sensing is still unknown. In fact, neurons activated by radial stretch and hypotonic stimuli seem to express TRESK, as they are sensitive to hydroxy-α-sanshool, a TRESK blocker (Bhattacharya *et al.*, 2008). These neurons were initially classified as LTMR or non-peptidergic nociceptors, which is in agreement with the TRESK expression pattern obtained from single-cell mRNA sequencing (Usoskin *et al.*, 2015).

In summary, we describe that genetic removal of TRESK specifically enhances mechanical and cold sensitivity in mice, not affecting the sensitivity to other stimuli. The development of specific TRESK openers/activators would be worthwhile to improve mechanical hypersensitivity and cold allodynia during chronic pain conditions.

Authors' contributions

Authors AC, AAB and GC performed electrophysiological recordings in neurons and calcium imaging. AC, APC and AAB performed behavioral experiments. AC, AAB carried out primary cell cultures. AC, GC, APC and NC performed qPCR experiments. AN and JN performed skin-nerve recordings. AC, DS, JN, NC and XG participated in the design of the study and performed the statistical analysis. XG conceived the study, oversaw the research and prepared the manuscript with help from all others. All authors read and approved the final manuscript.

Funding

Supported by grants from Ministerio de Economia y Competitividad and Instituto de Salud Carlos III/FEDER of Spain FIS PI14/00141 (XG), FIS PI17/00296 (XG), RETICs Oftared RD16/0008/0014 (XG), Generalitat de Catalunya 2017SGR737 (XG) and Ministerio de Economia, Industria y Competitividad, Spain (BFU2017-83317-P (DS).

Conflict of interest statement

The authors have no conflicts of interest to declare.

References

Abbott FV, Franklin KB & Westbrook RF (1995). The formalin test: scoring properties of the first and second phases of the pain response in rats. *Pain* **60,** 91–102.

Acosta C, Djouhri L, Watkins R, Berry C, Bromage K & Lawson SN (2014). TREK2 Expressed Selectively in IB4-Binding C-Fiber Nociceptors Hyperpolarizes Their Membrane Potentials and Limits Spontaneous Pain. *J Neurosci* **34,** 1494–1509.

Alessandri-Haber N, Joseph E, Dina OA, Liedtke W & Levine JD (2005). TRPV4 mediates pain-related behavior induced by mild hypertonic stimuli in the presence of inflammatory mediator. *Pain* **118,** 70–79.

Alessandri-Haber N, Yeh JJ, Boyd AE, Parada CA, Chen X, Reichling DB & Levine JD (2003). Hypotonicity induces TRPV4-mediated nociception in rat. *Neuron* **39,** 497–511.

Alloui A, Zimmermann K, Mamet J, Duprat F, Noël J, Chemin J, Guy N, Blondeau N, Voilley N, Rubat-Coudert C, Borsotto M, Romey G, Heurteaux C, Reeh P, Eschalier A & Lazdunski M (2006). TREK-1, a K+ channel involved in polymodal pain perception. *EMBO J* **25,** 2368–2376.

Bautista DM, Siemens J, Glazer JM, Tsuruda PR, Basbaum AI, Stucky CL, Jordt S-E & Julius D (2007). The menthol receptor TRPM8 is the principal detector of environmental cold. *Nature* **448,** 204–208.

Bautista DM, Sigal YM, Milstein AD, Garrison JL, Zorn JA, Tsuruda PR, Nicoll RA & Julius D (2008). Pungent agents from Szechuan peppers excite sensory neurons by inhibiting two-pore potassium channels. *Nat Neurosci* **11,** 772–779.

Beaulieu-Laroche L, Christin M, Donoghue A, Agosti F, Yousefpour N, Petitjean H, Davidova A, Stanton C, Khan U, Dietz C, Faure E, Fatima T, MacPherson A, Ribeiro-da-Silva A, Bourinet E, Blunck R & Sharif-Naeini R (2018). TACAN is an essential component of the mechanosensitive ion channel responsible for pain sensing. *bioRxiv*338673.

Bhattacharya MRC, Bautista DM, Wu K, Haeberle H, Lumpkin EA & Julius D (2008). Radial stretch reveals distinct populations of mechanosensitive mammalian somatosensory neurons. *Proc Natl Acad Sci U S A* **105,** 20015–20020.

Brenner DS, Golden JP & Gereau RW IV (2012). A novel behavioral assay for measuring cold sensation in mice. *PLoS ONE* **7,** e39765.

Callejo G, Castellanos A, Castany M, Gual A, Luna C, Acosta MC, Gallar J, Giblin JP & Gasull X (2015). Acid-sensing ion channels detect moderate acidifications to induce ocular pain. *Pain* **156,** 483–495.

Callejo G, Giblin JP & Gasull X (2013). Modulation of TRESK background K+

channel by membrane stretch. ed. Ceña V. *PLoS ONE* **8,** e64471.

Castellanos A, Andres-Bilbe A, Bernal L, Callejo G, Comes N, Gual A, Giblin JP, Roza C & Gasull X (2018). Pyrethroids inhibit K2P channels and activate sensory neurons. *Pain* **159,** 92–105.

Cavanaugh DJ, Lee H, Lo L, Shields SD, Zylka MJ, Basbaum AI & Anderson DJ (2009). Distinct subsets of unmyelinated primary sensory fibers mediate behavioral responses to noxious thermal and mechanical stimuli. *Proc Natl Acad Sci U S A* **106,** 9075–9080.

Chae YJ, Zhang J, Au P, Sabbadini M, Xie G-X & Yost CS (2010). Discrete change in volatile anesthetic sensitivity in mice with inactivated tandem pore potassium ion channel TRESK. *Anesthesiology* **113,** 1326–1337.

Chaplan SR, Bach FW, Pogrel JW, Chung JM & Yaksh TL (1994). Quantitative assessment of tactile allodynia in the rat paw. *J Neurosci Methods* **53,** 55–63.

Chiu IM, Barrett LB, Williams EK, Strochlic DE, Lee S, Weyer AD, Lou S, Bryman G, Roberson DP, Ghasemlou N, Piccoli C, Ahat E, Wang V, Cobos EJ, Stucky CL, Ma Q, Liberles SD & Woolf C (2014). Transcriptional profiling at whole population and single cell levels reveals somatosensory neuron molecular diversity. *Elife*; DOI: 10.7554/eLife.04660.

Czirják G & Enyedi P (2010). TRESK background K(+) channel is inhibited by phosphorylation via two distinct pathways. *Journal of Biological Chemistry* **285,** 14549–14557.

Descoeur J, Pereira V, Pizzoccaro A, Francois A, Ling B, Maffre V, Couette B, Busserolles J, Courteix C, Noël J, Lazdunski M, Eschalier A, Authier N & Bourinet E (2011). Oxaliplatin-induced cold hypersensitivity is due to remodelling of ion channel expression in nociceptors. *EMBO Mol Med* **3,** 266–278.

Dhandapani R, Arokiaraj CM, Taberner FJ, Pacifico P, Raja S, Nocchi L, Portulano C, Franciosa F, Maffei M, Hussain AF, de Castro Reis F, Reymond L, Perlas E, Garcovich S, Barth S, Johnsson K, Lechner SG & Heppenstall PA (2018). Control of mechanical pain hypersensitivity in mice through ligand-targeted photoablation of TrkB-positive sensory neurons. *Nature Communications* **9,** 1640.

Dobler T, Springauf A, Tovornik S, Weber M, Schmitt A, Sedlmeier R, Wischmeyer E & Döring F (2007). TRESK two-pore-domain K+ channels constitute a significant component of background potassium currents in murine dorsal root ganglion neurones. *J Physiol (Lond)* **585,** 867–879.

Du X, Gao H, Jaffe D, Zhang H & Gamper N (2018). M-type K +channels in peripheral nociceptive pathways. *British Journal of Pharmacology* **175,** 2158–2172.

Enyedi P & Czirják G (2010). Molecular background of leak K+ currents: two-

pore domain potassium channels. *Physiological Reviews* **90,** 559–605.

Fischer M, Carli G, Raboisson P & Reeh P (2013). The interphase of the formalin test. *Pain* **155,** 511–521.

Flegel C, Schöbel N, Altmüller J, Becker C, Tannapfel A, Hatt H & Gisselmann G (2015). RNA-Seq Analysis of Human Trigeminal and Dorsal Root Ganglia with a Focus on Chemoreceptors. *PLoS ONE* **10,** e0128951.

Gong J, Liu J, Ronan EA, He F, Cai W, Fatima M, Zhang W, Lee H, Li Z, Kim G-H, Pipe KP, Duan B, Liu J & Xu XZS (2019). A Cold-Sensing Receptor Encoded by a Glutamate Receptor Gene. *Cell* **178,** 1375–1386.e11.

Guo Z & Cao Y-Q (2014). Over-expression of TRESK K(+) channels reduces the excitability of trigeminal ganglion nociceptors. *PLoS ONE* **9,** e87029.

Guo Z, Qiu C-S, Jiang X, Zhang J, Li F, Liu Q, Dhaka A & Cao Y-Q (2019). TRESK K+ Channel Activity Regulates Trigeminal Nociception and Headache. *eNeuro*; DOI: 10.1523/ENEURO.0236-19.2019.

Julius D (2013). TRP channels and pain. *Annu Rev Cell Dev Biol* **29,** 355–384.

Kang D & Kim D (2006). TREK-2 (K2P10.1) and TRESK (K2P18.1) are major background K+ channels in dorsal root ganglion neurons. *Am J Physiol, Cell Physiol* **291,** C138–C146.

Kollert S, Dombert B, Döring F & Wischmeyer E (2015). Activation of TRESK channels by the inflammatory mediator lysophosphatidic acid balances nociceptive signalling. *Sci Rep* **5,** 12548.

Lafrenière RG et al. (2010). A dominant-negative mutation in the TRESK potassium channel is linked to familial migraine with aura. *Nat Med* **16,** 1157–1160.

LaPaglia DM, Sapio MR, Burbelo PD, Thierry-Mieg J, Thierry-Mieg D, Raithel SJ, Ramsden CE, Iadarola MJ & Mannes AJ (2018). RNA-Seq investigations of human post-mortem trigeminal ganglia. *Cephalalgia* **38,** 912–932.

Le Pichon CE & Chesler AT (2014). The functional and anatomical dissection of somatosensory subpopulations using mouse genetics. *Front Neuroanat* **8,** 21.

Li C-L, Li K-C, Wu D, Chen Y, Luo H, Zhao J-R, Wang S-S, Sun M-M, Lu Y-J, Zhong Y-Q, Hu X-Y, Hou R, Zhou B-B, Bao L, Xiao H-S & Zhang X (2016). Somatosensory neuron types identified by high-coverage single-cell RNA-sequencing and functional heterogeneity. *Cell Res* **26,** 83–102.

Lolignier S, Gkika D, Andersson D, Leipold E, Vetter I, Viana F, Noël J & Busserolles J (2016). New Insight in Cold Pain: Role of Ion Channels, Modulation, and Clinical Perspectives. *J Neurosci* **36,** 11435–11439.

Lu R, Lukowski R, Sausbier M, Zhang DD, Sisignano M, Schuh C-D, Kuner R, Ruth P, Geisslinger G & Schmidtko A (2013). BKCa channels expressed in sensory neurons modulate inflammatory pain in mice. *Pain* **155,** 556–565.

Ma C, Shu Y, Zheng Z, Chen Y, Yao H, Greenquist KW, White FA & LaMotte RH (2003). Similar electrophysiological changes in axotomized and neighboring intact dorsal root ganglion neurons. *J Neurophysiol* **89,** 1588–1602.

Madrid R, la Peña de E, Donovan-Rodriguez T, Belmonte C & Viana F (2009). Variable threshold of trigeminal cold-thermosensitive neurons is determined by a balance between TRPM8 and Kv1 potassium channels. *J Neurosci* **29,** 3120–3131.

Manteniotis S, Lehmann R, Flegel C, Vogel F, Hofreuter A, Schreiner BSP, Altmüller J, Becker C, Schöbel N, Hatt H & Gisselmann G (2013). Comprehensive RNA-Seq Expression Analysis of Sensory Ganglia with a Focus on Ion Channels and GPCRs in Trigeminal Ganglia ed. Zhang Z. *PLoS ONE* **8,** e79523.

Marsh B, Acosta C, Djouhri L & Lawson SN (2012). Leak K^+ channel mRNAs in dorsal root ganglia: relation to inflammation and spontaneous pain behaviour. *Molecular and cellular neurosciences* **49,** 375–386.

McNamara CR, Mandel-Brehm J, Bautista DM, Siemens J, Deranian KL, Zhao M, Hayward NJ, Chong JA, Julius D, Moran MM & Fanger CM (2007). TRPA1 mediates formalin-induced pain. *Proc Natl Acad Sci USA* **104,** 13525–13530.

Memon T, Chase K, Leavitt LS, Olivera BM & Teichert RW (2017). TRPA1 expression levels and excitability brake by KV channels influence cold sensitivity of TRPA1-expressing neurons. *Neuroscience* **353,** 76–86.

Morenilla-Palao C, Luis E, Fernández-Peña C, Quintero E, Weaver JL, Bayliss DA & Viana F (2014). Ion Channel Profile of TRPM8 Cold Receptors Reveals a Role of TASK-3 Potassium Channels in Thermosensation. *Cell Rep* **8,** 1571–1582.

Murthy SE, Loud MC, Daou I, Marshall KL, Schwaller F, Kühnemund J, Francisco AG, Keenan WT, Dubin AE, Lewin GR & Patapoutian A (2018). The mechanosensitive ion channel Piezo2 mediates sensitivity to mechanical pain in mice. *Sci Transl Med* **10,** eaat9897.

Nguyen MQ, Wu Y, Bonilla LS, Buchholtz von LJ & Ryba NJP (2017). Diversity amongst trigeminal neurons revealed by high throughput single cell sequencing ed. Obukhov AG. *PLoS ONE* **12,** e0185543–22.

Noël J, Zimmermann K, Busserolles J, Deval E, Alloui A, Diochot S, Guy N, Borsotto M, Reeh P, Eschalier A & Lazdunski M (2009). The mechano-activated K+ channels TRAAK and TREK-1 control both warm and cold perception. *EMBO J* **28,** 1308–1318.

Patel AJ, Honoré E, Maingret F, Lesage F, Fink M, Duprat F & Lazdunski M (1998). A mammalian two pore domain mechano-gated S-like K+ channel. *EMBO J* **17,** 4283–4290.

Pereira V, Busserolles J, Christin M, Devilliers M, Poupon L, Legha W, Alloui A, Aissouni Y, Bourinet E, Lesage F, Eschalier A, Lazdunski M & Noel J (2014). Role of the TREK2 potassium channel in cold and warm thermosensation and in pain perception. *Pain* **155,** 2534–2544.

Ranade SS, Woo S-H, Dubin AE, Moshourab RA, Wetzel C, Petrus M, Mathur J, Bégay V, Coste B, Mainquist J, Wilson AJ, Francisco AG, Reddy K, Qiu Z, Wood JN, Lewin GR & Patapoutian A (2014). Piezo2 is the major transducer of mechanical forces for touch sensation in mice. *Nature* **516,** 121–125.

Ray P, Torck A, Quigley L, Wangzhou A, Neiman M, Rao C, Lam T, Kim J-Y, Kim TH, Zhang MQ, Dussor G & Price TJ (2018). Comparative transcriptome profiling of the human and mouse dorsal root ganglia: an RNA-seq-based resource for pain and sensory neuroscience research. *Pain* **159,** 1325–1345.

Royal P, Andres-Bilbe A, Ávalos Prado P, Verkest C, Wdziekonski B, Schaub S, Baron A, Lesage F, Gasull X, Levitz J & Sandoz G (2019). Migraine-Associated TRESK Mutations Increase Neuronal Excitability through Alternative Translation Initiation and Inhibition of TREK. *Neuron* **101,** 232–245.e236.

Story GM, Peier AM, Reeve AJ, Eid SR, Mosbacher J, Hricik TR, Earley TJ, Hergarden AC, Andersson DA, Hwang SW, McIntyre P, Jegla T, Bevan S & Patapoutian A (2003). ANKTM1, a TRP-like channel expressed in nociceptive neurons, is activated by cold temperatures. *Cell* **112,** 819–829.

Szczot M, Liljencrantz J, Ghitani N, Barik A, Lam R, Thompson JH, Bharucha-Goebel D, Saade D, Necaise A, Donkervoort S, Foley AR, Gordon T, Case L, Bushnell MC, Bönnemann CG & Chesler AT (2018). PIEZO2 mediates injury-induced tactile pain in mice and humans. *Sci Transl Med* **10,** eaat9892.

Tjølsen A, Berge OG, Hunskaar S, Rosland JH & Hole K (1992). The formalin test: an evaluation of the method. *Pain* **51,** 5–17.

Tulleuda A, Cokic B, Callejo G, Saiani B, Serra J & Gasull X (2011). TRESK channel contribution to nociceptive sensory neurons excitability: modulation by nerve injury. *Mol Pain* **7,** 30.

Usoskin D, Furlan A, Islam S, Abdo H, Lönnerberg P, Lou D, Hjerling-Leffler J, Haeggström J, Kharchenko O, Kharchenko PV, Linnarsson S & Ernfors P (2015). Unbiased classification of sensory neuron types by large-scale single-cell RNA sequencing. *Nat Neurosci* **18,** 145–153.

Vriens J, Nilius B & Voets T (2014). Peripheral thermosensation in mammals. *Nat Rev Neurosci* **15,** 573–589.

Weir GA, Pettingill P, Wu Y, Duggal G, Ilie A-S, Akerman CJ & Cader MZ (2019). The Role of TRESK in Discrete Sensory Neuron Populations and Somatosensory Processing. *Front Mol Neurosci* **12,** 170.

Winter Z, Gruschwitz P, Eger S, Touska F & Zimmermann K (2017). Cold Temperature Encoding by Cutaneous TRPA1 and TRPM8-Carrying Fibers in the Mouse. *Front Mol Neurosci* **10,** 209.

Yalcin I, Charlet A, Freund-Mercier M-J, Barrot M & Poisbeau P (2009). Differentiating Thermal Allodynia and Hyperalgesia Using Dynamic Hot and Cold Plate in Rodents. *The Journal of Pain* **10,** 767–773.

Yalcin I, Megat S, Barthas F, Waltisperger E, Kremer M, Salvat E & Barrot M (2014). The sciatic nerve cuffing model of neuropathic pain in mice. *J Vis Exp*; DOI: 10.3791/51608.

Yamamoto Y, Hatakeyama T & Taniguchi K (2009). Immunohistochemical colocalization of TREK-1, TREK-2 and TRAAK with TRP channels in the trigeminal ganglion cells. *Neurosci Lett* **454,** 129–133.

Yang Y, Li S, Jin Z-R, Jing H-B, Zhao H-Y, Liu B-H, Liang Y-J, Liu L-Y, Cai J, Wan Y & Xing G-G (2018). Decreased abundance of TRESK two-pore domain potassium channels in sensory neurons underlies the pain associated with bone metastasis. *Sci Signal* **11,** eaao5150.

Yarmolinsky DA, Peng Y, Pogorzala LA, Rutlin M, Hoon MA & Zuker CS (2016). Coding and Plasticity in the Mammalian Thermosensory System. *Neuron* **92,** 1079–1092.

Zeisel A et al. (2018). Molecular Architecture of the Mouse Nervous System. *Cell* **174,** 999–1014.e22.

Zheng Y, Liu P, Bai L, Trimmer JS, Bean BP & Ginty DD (2019). Deep Sequencing of Somatosensory Neurons Reveals Molecular Determinants of Intrinsic Physiological Properties. *Neuron* **103,** 598–616.e7.

Zhou J, Yang C-X, Zhong J-Y & Wang H-B (2013). Intrathecal TRESK gene recombinant adenovirus attenuates spared nerve injury-induced neuropathic pain in rats. *Neuroreport* **24,** 131–136.

Zhou J, Yao S-L, Yang C-X, Zhong J-Y, Wang H-B & Zhang Y (2012). TRESK gene recombinant adenovirus vector inhibits capsaicin-mediated substance P release from cultured rat dorsal root ganglion neurons. *Mol Med Report* **5,** 1049–1052.

Zimmermann K, Hein A, Hager U, Kaczmarek JS, Turnquist BP, Clapham DE & Reeh PW (2009). Phenotyping sensory nerve endings in vitro in the mouse. *Nat Protoc* **4,** 174–196.

Figure Legends

Figure 1: Nociceptive sensory neurons lacking TRESK have a decreased standing outward current.

A. Expression profile of K_{2P} channels, TRPA1 and TRPV1 in mouse sensory neurons from wild-type and TRESK knockout mice. mRNA expression obtained by quantitative PCR shows no significant differences between WT and KO animals after genetic deletion of TRESK. Y-axis shows the ΔCt (number of cycles target - number of cycles GADPH) for the different mRNAs. Notice that the Y-axis has been inverted to visually show that lower ΔCt numbers are indicative of a higher expression. Each dot represents a single animal (wild-type n=6; TRESK knockout n=7). **B.** Top: Representative recordings of whole-cell currents from small-sized DRG sensory neurons using a protocol to minimize activation of voltage-gated transient K^+ outward currents (holding voltage -60mV). Bottom: quantification of currents at the end of the pulse (mean±SD) at -25 mV (a) and at the end of the ramp (-135 mV; b) showed significant differences among groups (*p<0.05; **p<0.01 unpaired t-test. wild-type n=31; TRESK KO n=50).

Figure 2: Nociceptive sensory neurons lacking TRESK present a higher excitability

A. Representative whole-cell current-clamp recordings from wild-type and TRESK knockout nociceptive sensory neurons elicited by hyperpolarizing or depolarizing 400 ms current pulses in 10 pA increments from -50 pA. *Right*: mean membrane capacitance (C_m) from neurons studied is shown. **B.** Quantification of the electrophysiological parameters analyzed in wild-type

(black bars, n=13) and TRESK KO (red bars, n=27) sensory neurons. RMP: resting membrane potential. Rheobase was measured using 400 ms depolarizing current pulses in 10 pA increments; R_{in}: whole-cell input resistance was calculated on the basis of the steady-state I-V relationship during a series of 400 ms hyperpolarizing currents delivered in steps of 10 pA from -50 to -10 pA. AP amplitude was measured from the RMP to the AP peak. AP duration/width was measured at 50% of the AP amplitude. Data is presented as mean±SD. Statistical differences between groups are shown (*p<0.05, **p<0.01 unpaired t-test). **C.** Examples and quantification of neuronal excitability as the number of action potentials fired in response to a depolarizing current ramp (0 to 500 pA, 1s) from a holding voltage of -60 mV (black, wild-type n=10; red, TRESK KO n=18). The peak to peak interspike interval value between the four initial action potentials was measured and averaged. Statistical differences between groups are shown (*p<0.05; **p<0.01 unpaired t-test).

Figure 3: TRESK KO mice present diminished responses to osmotic stimuli and TRPA1 activation.

A. Representative recordings of intracellular calcium (Fura-2 ratiometric imaging) of wild-type or TRESK KO DRG sensory neurons exposed to menthol (100 μM), allyl isothiocyanate (AITC, 100 μM) and capsaicin (1 μM). Venn diagrams show the relative size and overlap between the populations of neurons activated by each agonist. Number of total cells analyzed was 1124 (wild-type) and 1228 (knock-out). The number of responding cells in each subgroup is shown in parenthesis. Non-responding neurons to any of the agonists assayed were 246 (wild-type) and 446 (knock-out). **B.** Quantification of

the percentage of neurons responding to each agonist in intracellular calcium recordings. Statistical differences between groups are shown (**p<0.01 unpaired t-test). **C.** Nocifensive behavior: quantification of the time the animals spent licking and shaking the paw after intradermal injection of AITC (10%) or capsaicin (1µg/10µl) in the hind paw for wild-type and TRESK knockout mice. The mean time spent showing nocifensive behaviors over a period of 5 min is shown (WT n=13; KO n=13 animals). **D.** Formalin-induced pain: *Top*. Time course of licking/shaking behavior directed to the formalin-injected hind paw. *Bottom*: quantification of cumulative time spent in phase I (0-10 min), IIa (11-30 min) and IIb (31 to 50 min). n= 5-6 animals per group. **E.** Osmotic pain: quantification of the time spent licking and shaking the paw after intradermal injection of hypotonic (-33%) or hypertonic (2% and 10%) stimuli in the hind paw of wild-type and TRESK knockout mice. The mean time spent showing nocifensive behaviors over a period of 5 min is shown. 6 to 11 animals were evaluated in each group. When indicated, a 5 µl-injection of prostaglandin E_2 (PGE_2) was injected in the hind paw of each mouse 30 min before the test to sensitize nociceptors. Statistical differences are shown as *p<0.05, **p<0.01 (Student's unpaired t-test) between WT and KO mice.

Figure 4: TRESK-lacking mice present mechanical allodynia and normal heat sensitivity

A. Mechanical threshold obtained with von Frey hairs from saphenous nerve C-fibers. *Left.* Distribution of von Frey thresholds. Mean±SD is shown (black lines). Geometric mean is indicated as a blue line. Wild-type n=14, knock-out n=22. *Right*. Magnification of 0-25 mN range of von Frey Thresholds to highlight the

larger distribution of fibers from KO mouse to lower threshold values. **B.** Mechanical sensitivity. *Left*: von Frey response thresholds obtained with the up and down method in male and female wild-type and TRESK knockout animals (male WT n=58, KO n=33; female WT n=18, KO n=19). *Right*: latency to hind paw withdrawal in the dynamic plantar test (male WT n=27; KO n=22). Statistical differences are shown as *p<0.05, ***p<0.001 (Student's unpaired t-test) between WT and KO mice. **C.** *Left.* Distribution of heat thresholds from C-fibers recorded from wild-type (n=35) and TRESK KO mice (n=37), measured in skin-nerve experiments. *Right.* Mean number of spikes fired by heat sensitive C-fibers during a heat-ramp from 30 to 50ºC. No significant differences were found. **D.** Heat sensitivity. *Left*: radiant heat (Hargreaves' test) in male (WT n=39; KO n=38); and female animals (WT n=18; KO n=15). *Right*: Noxious heat sensitivity to 52 and 56ºC (Hot plate test) in male (WT n=8/9; KO n=13/11); and female animals (WT n=9/9; KO n=12/8). **E.** Dynamic hot plate: in contrast to the conventional hot plate, the dynamic hot plate allows the testing of a wide range of temperatures. Plate temperature was ramped from 30ºC to 50ºC at a 1ºC/min rate. To determine the temperature that is perceived as noxious for mice and quantify pain-related behaviors, the number of jumps at each temperature was scored. *Left*: number of jumps elicited at each temperature in male and female wild-type and TRESK KO mice (n=11-15 animals per group). No significant differences were obtained between wild-type and TRESK (One-way ANOVA with Holm-Sidak correction). *Right:* mean temperature at which animals did the first jump (threshold) and total number of jumps for male and female mice in the whole range of temperatures. Values for temperatures between 30 and 38ºC

are not shown in the plots since were probably detected as non-noxious and did not produce any observable response.

Figure 5: Cold allodynia in TRESK deleted mice

A. Fractions of cold-sensitive C-fibers in WT (total number of C-fibers = 35) and TRESK KO (n=37 C-fibers), measured in skin-nerve experiments. Numbers in bars are the percentage of Mechano-Heat-Cold (C-MHC) and Mechano-Cold (C-MC) fibers. A significant difference in the distribution of cold fibers is shown (**p<0.01, Chi-square test). **B.** Distribution of the C-fibers activated by cold at different temperatures between WT and KO animals. **C.** Distribution of cold thresholds from fibers recorded (WT n=19; KO n=38). Mean and SD are shown. **D.** Representative experiments of C-fibers activated by a cold ramp. *Top*. Action potentials (Spikes) fired in response to a temperature decrease are shown for wild-type and a TRESK knockout cold C-fibers. The average action potential is presented on the right. A representative cold ramp from 30 to 10°C is shown below. *Bottom*: Histogram of mean responses to cooling, 5-second bin, of C-fibers from wild-type and TRESK KO mice. **E, F.** Cold sensitivity measured with the cold plate (2ºC) and cold plantar assays in male and female wild-type and TRESK knockout animals (n=11-19 animals per group). **G.** Cold avoidance measured in the thermal place preference test. The percentage of time spent at the reference plate (30ºC) at each experimental temperature is shown (n=8-14 male animals per group). Statistical differences are shown as *p<0.05, **p<0.01, ***p<0.001 with Student's unpaired t-test (E,F) or one-way ANOVA plus Holm-Sidak correction for multiple comparisons (G) between WT and KO mice.

Figure 6: Changes in chronic pain in TRESK-deleted mice

A. Mechanical and thermal sensitivity in the CFA-induced inflammatory pain model. Mechanical sensitivity was measured with von Frey filaments (up and down method) and thermal sensitivity was measured with the Hargreaves test (n=7 animals CFA groups; 5 animals vehicle groups) **B.** Mechanical and thermal sensitivity in the cuff-induced neuropathic pain model. Mechanical sensitivity was measured with von Frey filaments (up and down method) and thermal sensitivity was measured with the Hargreaves test (n=6 animals in each group). **C.** Oxaliplatin-induced cold sensitization model. *Left.* Paw withdrawal latency to the cold plantar assay before (baseline) and 90h after oxaliplatin injection in WT and TRESK KO animals (n=9 and 10 animals per group). *Right.* Cold avoidance measured in the thermal place preference test. The percentage of time spent at the reference plate (30ºC) versus the experimental temperature (20ºC) is shown (n=6 and 8 animals per group). Statistical differences between WT and KO mice are shown as *p<0.05, **p<0.01, ***p<0.001. Two-way ANOVA plus Holm-Sidak correction for multiple comparisons (data on panels A and B) or Student's paired t-test (panel C; baseline vs. oxaliplatin) were used.

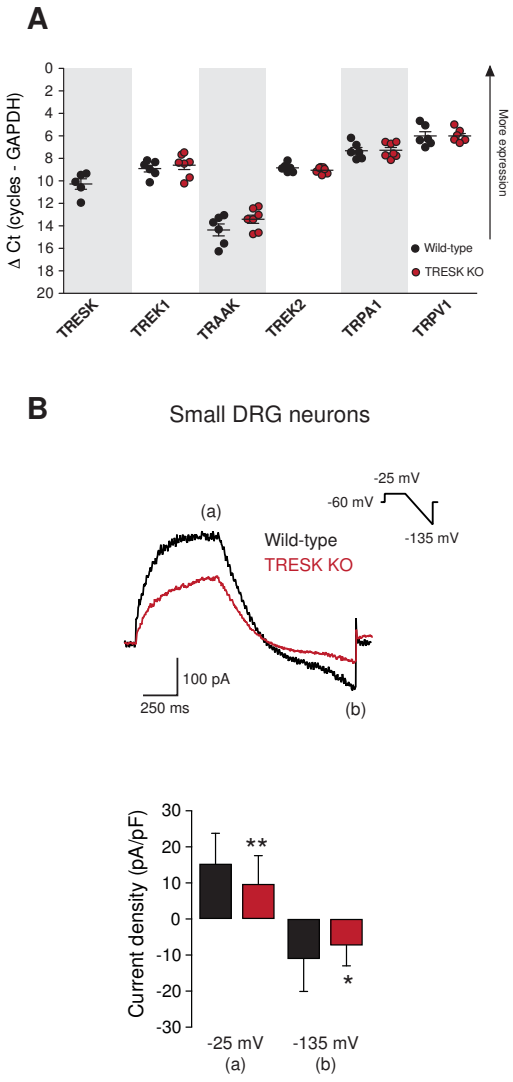
A
Δ Ct (cycles - GAPDH)
0
2
4
6
8
10
12
14
16
18
20
More expression
Wild-type
TRESK KO
TRESK
TREK1
TRAAK
TREK2
TRPA1
TRPV1
B
Small DRG neurons
-25 mV
-60 mV
-135 mV
(a)
Wild-type
TRESK KO
100 pA
250 ms
(b)
Current density (pA/pF)
30
20
10
0
-10
-20
-30
**
*
-25 mV
(a)
-135 mV
(b)

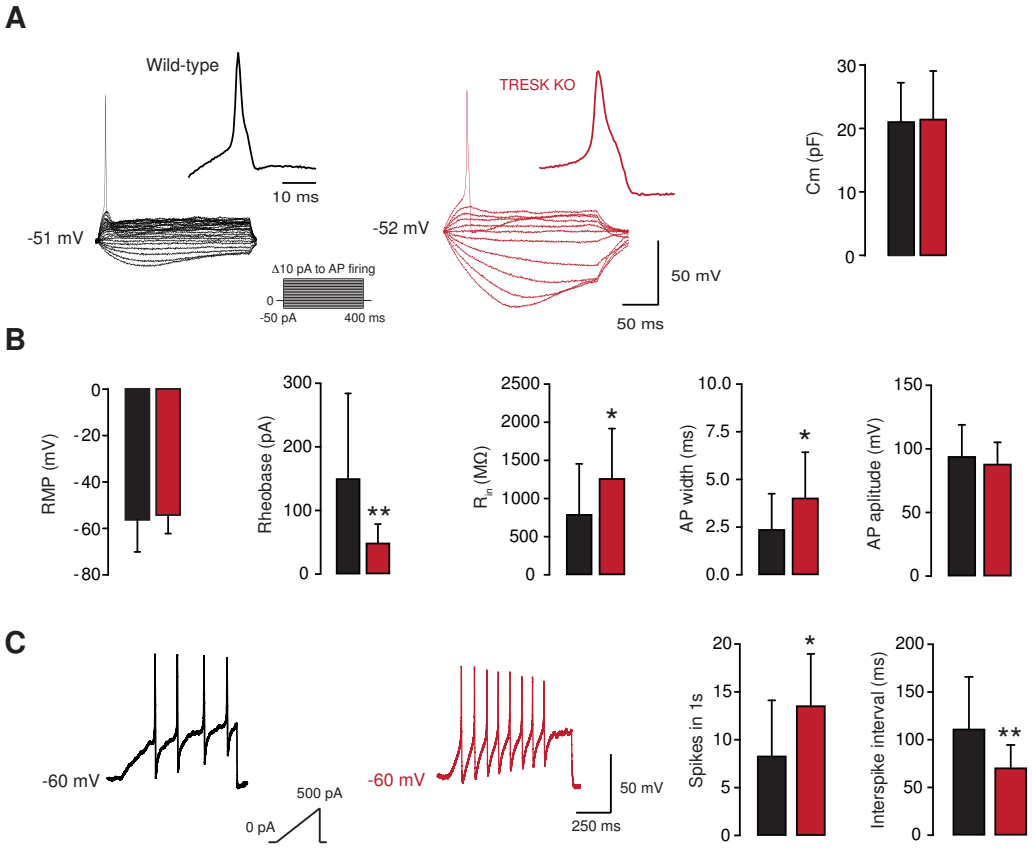
A
Wild-type
10 ms
-51 mV
Δ10 pA to AP firing
0
-50 pA
400 ms
TRESK KO
-52 mV
50 mV
50 ms
Cm (pF)
30
20
10
0
B
RMP (mV)
0
-20
-40
-60
-80
Rheobase (pA)
300
200
100
0
**
R_{in} (MΩ)
2500
2000
1500
1000
500
0
*
AP width (ms)
10.0
7.5
5.0
2.5
0.0
*
AP aplitude (mV)
150
100
50
0
C
-60 mV
500 pA
0 pA
-60 mV
50 mV
250 ms
Spikes in 1s
20
15
10
5
0
*
Interspike interval (ms)
200
150
100
50
0
**

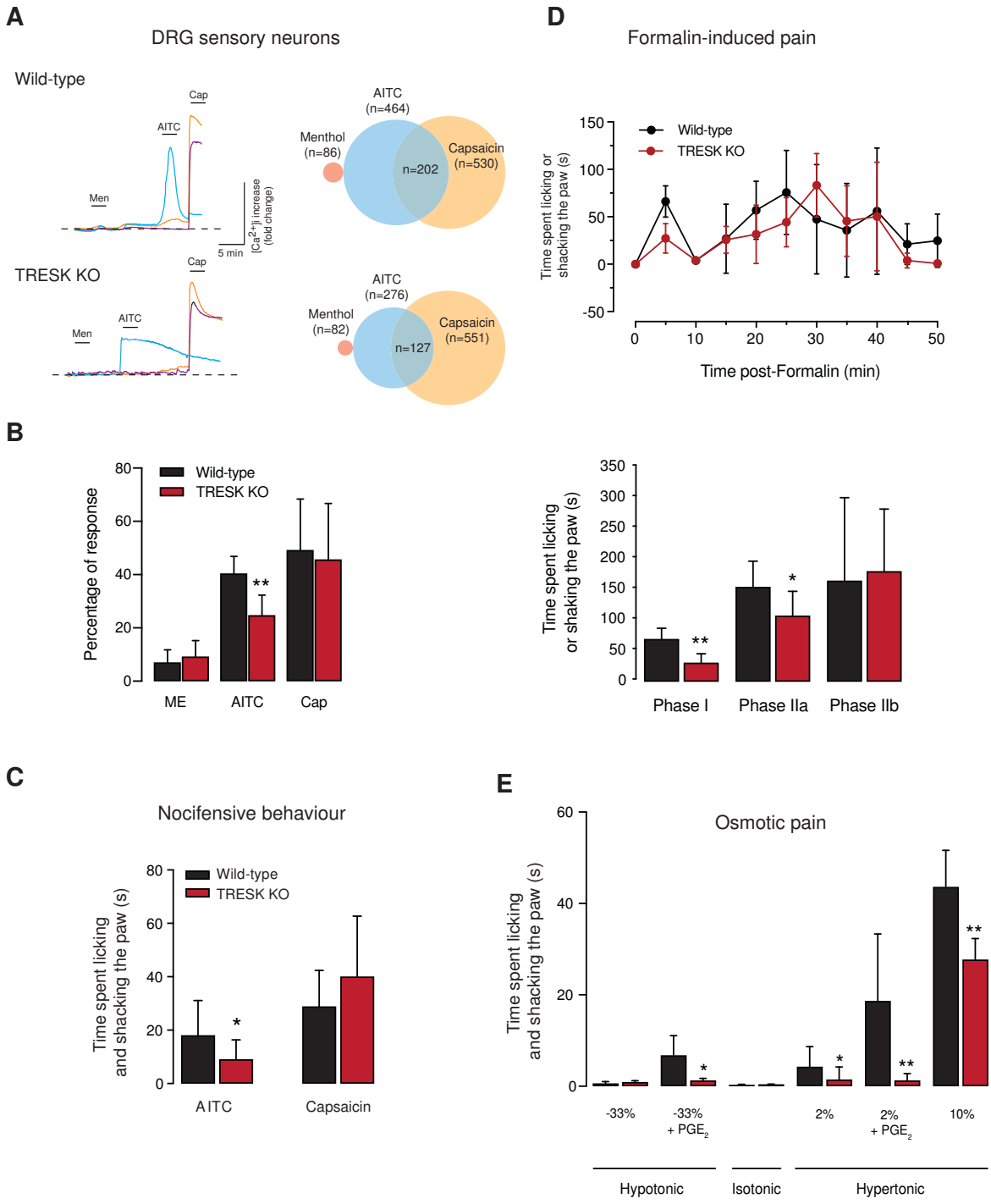
A
DRG sensory neurons
Wild-type
Cap
AITC
Men
5 min
[Ca2+]i increase (fold change)
AITC (n=464)
Menthol (n=86)
n=202
Capsaicin (n=530)
TRESK KO
Cap
AITC
Men
AITC (n=276)
Menthol (n=82)
n=127
Capsaicin (n=551)
D
Formalin-induced pain
Wild-type
TRESK KO
Time spent licking or shacking the paw (s)
Time post-Formalin (min)
B
Wild-type
TRESK KO
Percentage of response
ME
AITC
Cap
Time spent licking or shaking the paw (s)
Phase I
Phase IIa
Phase IIb
C
Nocifensive behaviour
Wild-type
TRESK KO
Time spent licking and shacking the paw (s)
AITC
Capsaicin
E
Osmotic pain
Time spent licking and shacking the paw (s)
-33%
-33% + PGE2
2%
2% + PGE2
10%
Hypotonic
Isotonic
Hypertonic

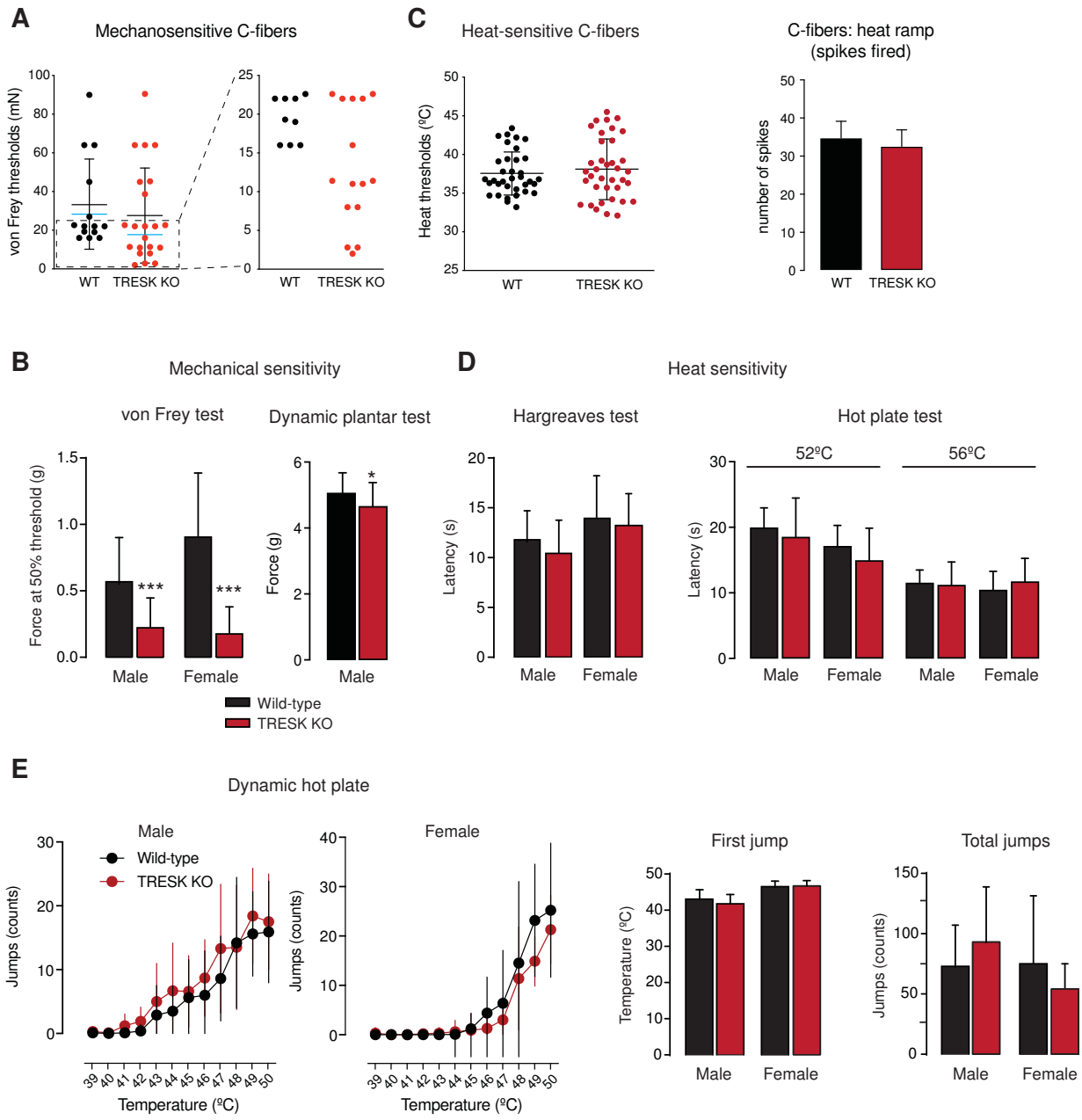
A
Mechanosensitive C-fibers
von Frey thresholds (mN)
WT
TRESK KO
C
Heat-sensitive C-fibers
Heat thresholds (ºC)
C-fibers: heat ramp
(spikes fired)
number of spikes
B
Mechanical sensitivity
von Frey test
Force at 50% threshold (g)
Dynamic plantar test
Force (g)
Male
Female
Wild-type
TRESK KO
D
Heat sensitivity
Hargreaves test
Latency (s)
Hot plate test
52ºC
56ºC
E
Dynamic hot plate
Jumps (counts)
Temperature (ºC)
First jump
Total jumps

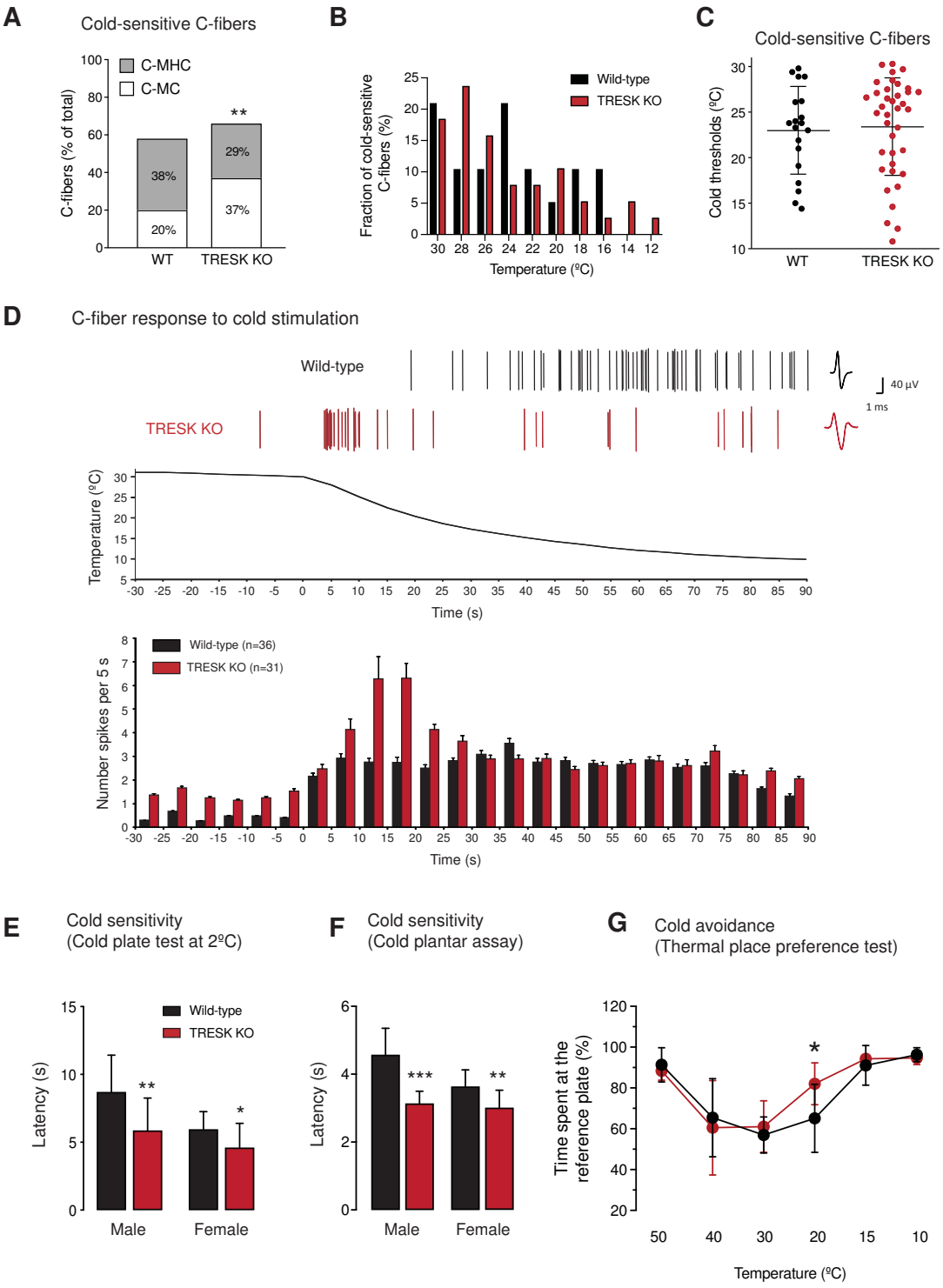
A
Cold-sensitive C-fibers
C-MHC
C-MC
C-fibers (% of total)
38%
20%
29%
37%
**
WT
TRESK KO
B
Fraction of cold-sensitive C-fibers (%)
Wild-type
TRESK KO
Temperature (ºC)
C
Cold-sensitive C-fibers
Cold thresholds (ºC)
WT
TRESK KO
D
C-fiber response to cold stimulation
Wild-type
TRESK KO
40 µV
1 ms
Temperature (ºC)
Time (s)
Wild-type (n=36)
TRESK KO (n=31)
Number spikes per 5 s
Time (s)
E
Cold sensitivity
(Cold plate test at 2ºC)
Wild-type
TRESK KO
Latency (s)
**
*
Male
Female
F
Cold sensitivity
(Cold plantar assay)
Latency (s)
***
**
Male
Female
G
Cold avoidance
(Thermal place preference test)
Time spent at the reference plate (%)
*
Temperature (ºC)

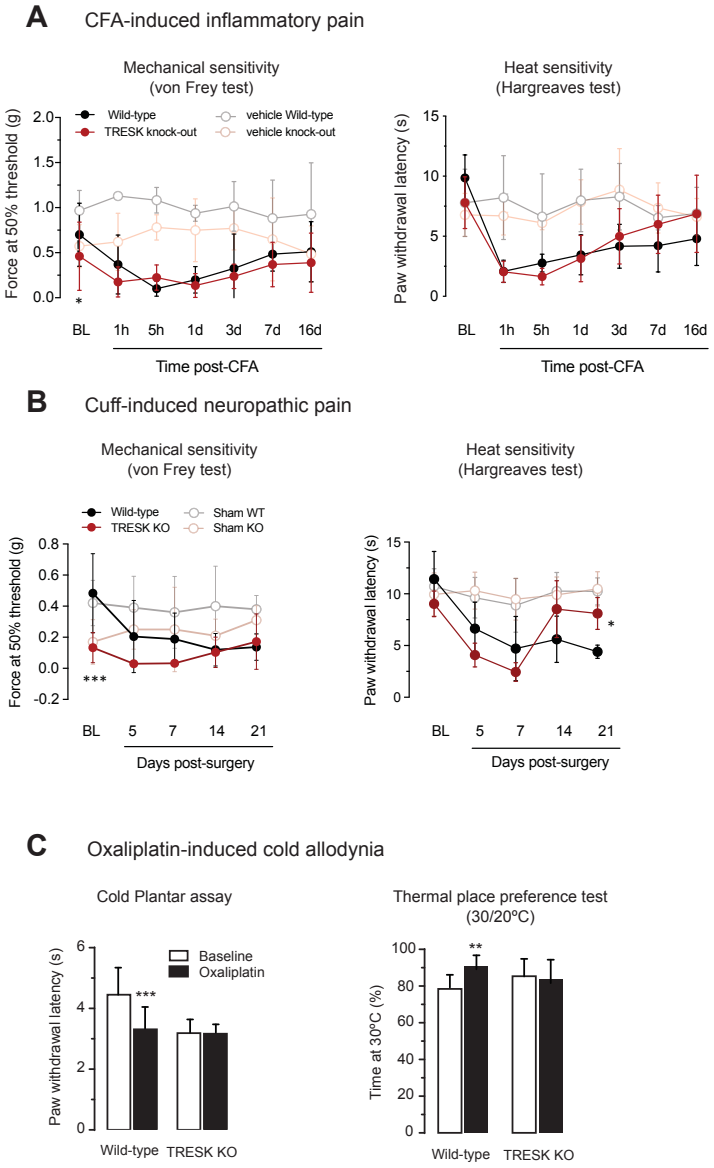
A
CFA-induced inflammatory pain
Mechanical sensitivity
(von Frey test)
Heat sensitivity
(Hargreaves test)
Wild-type
TRESK knock-out
vehicle Wild-type
vehicle knock-out
Force at 50% threshold (g)
Paw withdrawal latency (s)
BL
1h
5h
1d
3d
7d
16d
Time post-CFA
B
Cuff-induced neuropathic pain
Mechanical sensitivity
(von Frey test)
Heat sensitivity
(Hargreaves test)
Wild-type
TRESK KO
Sham WT
Sham KO
Force at 50% threshold (g)
Paw withdrawal latency (s)
BL
5
7
14
21
Days post-surgery
C
Oxaliplatin-induced cold allodynia
Cold Plantar assay
Thermal place preference test
(30/20ºC)
Baseline
Oxaliplatin
Paw withdrawal latency (s)
Time at 30ºC (%)
Wild-type
TRESK KO